ACCSCIENCE PUBLISHING

Tumor Discovery

REVIEW ARTICLE

Structural cell communities in the tumor microenvironment: Spatial determinants of therapeutic response

Xuan Cui, Yuanli Ni, Xia Lei, Lan Zhao, Cheng Qian*, and Juanjuan Shan*

Chongqing Key Laboratory of Translational Research for Cancer Metastasis and Individualized Treatment, Chongqing University Cancer Hospital, School of Medicine, Chongqing University, Chongqing, China

Abstract

Despite advances in cancer therapies, treatment responses remain highly variable due to the complexity and heterogeneity of the tumor microenvironment. The tumor microenvironment comprises malignant, immune, stromal, and endothelial cells, along with extracellular matrix and soluble factors, all organized into spatially distinct communities that evolve dynamically throughout tumor progression and therapy. These spatial structures orchestrate tumor behavior, immune evasion, and drug resistance. Recent breakthroughs in spatial omics technologies, including spatial transcriptomics and spatial proteomics, have enabled high-resolution, multiplexed mapping of tissue architecture and molecular characteristics. These technologies provide valuable insights into how the spatial organization of cells and signaling networks within the tumor microenvironment influences therapeutic efficacy. Notably, specific structures, such as tertiary lymphoid structures, fibroblast-mediated stromal barriers, and vascular heterogeneity have been identified as spatial determinants of treatment response. By delineating cellular communities and their interactions, spatial omics technologies can reduce intratumoral complexity into clinically interpretable modules. This review summarizes the diversity of these spatial structures and their relationships with treatment outcomes in immunotherapy, chemotherapy, radiotherapy, and targeted therapy. In addition, it highlights present challenges in data integration, analytical standardization, and functional validation, and discusses future directions for incorporating spatial omics technologies into precision medicine.

Keywords: Tumor microenvironment; Therapeutic response; Spatial heterogeneity; Cellular community; Spatial omics

***Corresponding authors:**
Juanjuan Shan| (juanjuansh@cqu.edu.cn);
Cheng Qian (cqian@cqu.edu.cn)

Citation: Cui X, Ni Y, Lei X, Zhao L, Qian C, Shan J. Structural cell communities in the tumor microenvironment: Spatial determinants of therapeutic response. *Tumor Discov*. 2025;4(4):34-55. doi: 10.36922/TD025250049

Received: June 20, 2025

Revised: July 16, 2025

Accepted: July 29, 2025

Published online: August 14, 2025

1. Introduction

Despite significant advances in cancer therapies over the past few decades, treatment outcomes remain highly variable. Many patients experience drug resistance or poor outcomes, primarily due to tumor heterogeneity and the complex tumor microenvironment (TME).[1] The TME—comprising malignant cells, immune cells, stromal cells, endothelial cells, extracellular matrix (ECM), and soluble factors—is highly diverse and spatially organized.[2] These cell types are further subdivided into

distinct subtypes, each exhibiting unique phenotypic and functional characteristics. Their complex crosstalk forms localized microenvironments that vary in cell composition, spatial distribution, signaling molecules, and metabolic state. The TME not only provides a supportive niche for tumor cells but also constructs a dynamic ecosystem that critically influences therapeutic responses. Consequently, a comprehensive understanding of the spatial and functional heterogeneity within the TME is essential for overcoming present treatment limitations.[3]

Recent advances in spatial omics technologies, such as imaging mass cytometry (IMC) and spatial transcriptomics (ST), have revolutionized the characterization of tissue architecture. These technologies enable the simultaneous capture of spatial structural information and the transcriptome, proteome, epigenome, or metabolome, offering pivotal insight into how tissue organization regulates tumor progression and therapeutic responses.[4,5] Over the past decade, continuous advancements in spatial resolution have established spatial omics as a critical tool in cancer research.[6]

Early multiplex immunofluorescence (mIF) technology enabled the visualization of multiple protein markers in tumor sections, supporting biomarker discovery and precision pathology.[7,8] The emergence of IMC in 2014 integrated mass spectrometry with metal-labeled antibodies to enable highly multiplexed protein profiling.[9] In 2016, ST technology allowed for the spatial mapping of gene expression at single-cell resolution.[10] In 2019, digital spatial profiling (DSP) was launched, integrating high-throughput analysis with optical labeling to enable precise protein and gene expression analysis in specific tissue regions.[11] Furthermore, the development of cyclic immunofluorescence,[12] CO-Detection by Indexing,[13] iterative bleaching and exchange,[14] multiplexed ion beam imaging,[15] and deep visual proteomics[16] has expanded the depth and breadth of spatial analysis. *Nature Methods* recognized spatial proteomics as the 2024 method of the year for its critical role in uncovering complex tissue structures.

These technological advances have uncovered critical spatial features of the TME that correlate with treatment response. For example, tertiary lymphoid structures (TLS), spatially organized immune cell aggregates, have emerged as predictive markers of immunotherapy outcomes across multiple cancers.[17-19] In addition, the spatial distribution of tumor-infiltrating lymphocytes, fibroblast barriers, and vascular patterns has been associated with therapeutic responses to chemotherapy, radiotherapy, and targeted therapy.[20-22] By capturing these cellular spatial relationships and the cellular communities formed in the TME, TME heterogeneity can be simplified into clinically recognizable entities, providing new perspectives for researchers in advancing cancer diagnosis, treatment, and drug development (Figure 1).

In this review, we systematically summarize how spatial omics technologies elucidate the composition and structural organization of the TME in various cancers, as well as their role in modulating responses to immunotherapy, targeted therapy, chemotherapy, and radiotherapy. These insights provide a foundation for the further optimization of cancer treatments and the development of precision oncology strategies.

2. Spatial immune communities and responses to immunotherapy

Building on foundational mouse studies, Schreiber *et al.*[23-26] demonstrated that tumor-infiltrating T cells significantly influence the progression and clinical behavior of human cancers,[27,28] thereby revolutionizing the field of tumor immunology. Hanahan and Weinberg[29] identified "evading immune destruction" as a new hallmark of cancer. Immunotherapy strategies are designed to restore or enhance the antitumor capacity of the host immune system,[30,31] including immune checkpoint inhibitors (ICI),[32] chimeric antigen receptor T cells,[33] cancer vaccines,[34] cytokine-based therapies,[35] and oncolytic viruses.[36]

However, patient responses to immunotherapy are highly heterogeneous. This variability reflects not only inter-individual immune differences but also the spatial organization of immune cells within the TME.[37] Immune cells may localize in distinct regions, including the tumor core (TC), invasive margins, or TLS, forming diverse immune niches that modulate therapeutic efficacy. This section summarizes how the density, proximity, and cellular interactions of immune communities influence the effectiveness of immunotherapy (Table 1).

2.1. T cell infiltration and density

Tumor-infiltrating lymphocytes, particularly cluster of differentiation (CD) 8^+ cytotoxic T cells, play critical roles in tumor immunotherapy. The functional state and density of $CD8^+$ T cells often determine the efficacy of ICIs.[74-76] In metastatic triple-negative breast cancer (TNBC), pembrolizumab responders exhibited significantly higher densities of pre-existing intratumoral $CD8^+$ T cells compared to non-responders, which were engaged in close interactions with tumor cells. Post-treatment responders also demonstrated reduced proximity between $CD8^+$ T cells and $CD15^+$ neutrophils, suggesting an escape from neutrophil-mediated immunosuppression.[38]

In patients with esophageal squamous cell carcinoma undergoing neoadjuvant immunochemotherapy,

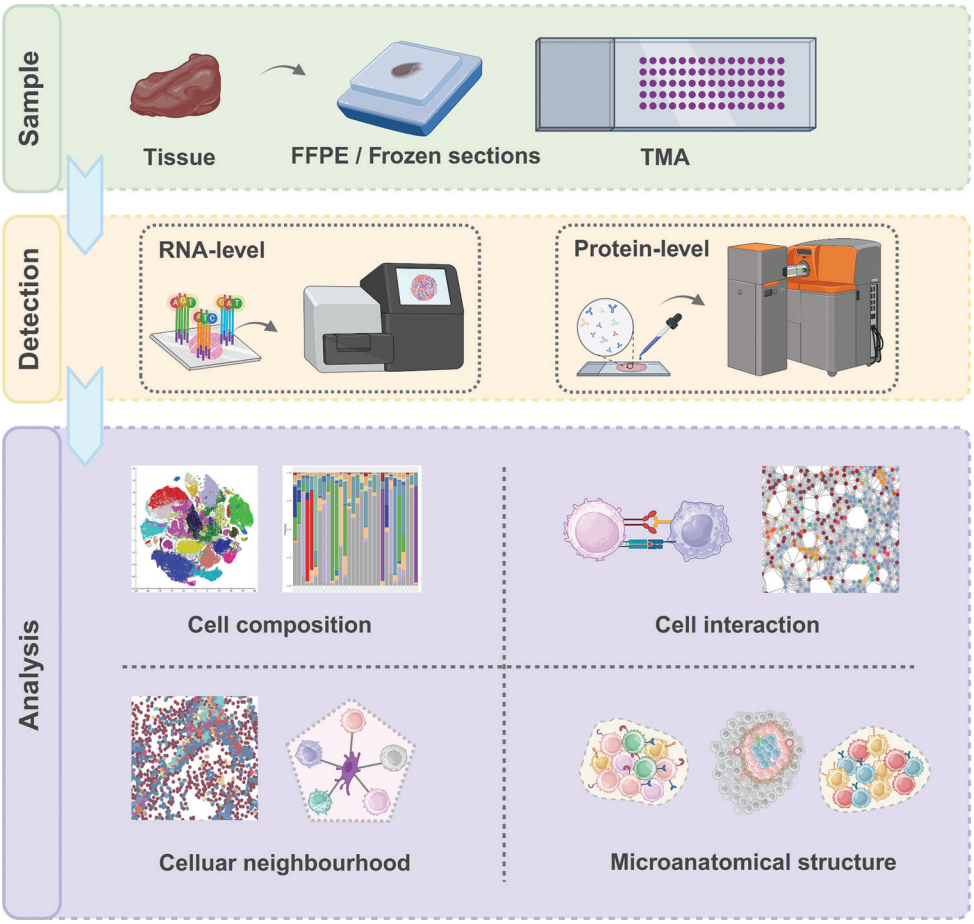

Figure 1. Comprehensive workflow for spatial-omics profiling of the tumor microenvironment. Fresh or frozen tumor specimens are processed into FFPE blocks or cryosectioned and arrayed into TMAs. Spatial omics platforms—spatial transcriptomics for RNA-level analysis, and imaging mass cytometry, multiplex immunofluorescence, or digital spatial profiling for proteinlevel interrogation—map molecular distributions within intact tissue architecture. Subsequent computational pipelines extract key spatial features: (i) Cell composition, through unsupervised clustering and quantitative deconvolution of discrete cell populations; (ii) cell-cell interactions, through inference of ligand-receptor signaling networks and spatial interaction graphs; (iii) cellular neighborhoods, by identifying local cooccurrence patterns and niche enrichment; and (iv) microanatomical structures, through reconstruction of higherorder tissue units, such as immune-stromal interfaces and tertiary lymphoid structures. The figure was created using Biorender.com. Shan, J. (2025) https://BioRender.com/rbaqcof.
Abbreviations: FFPE: Formalinfixed, paraffinembedded; TMA: Tissue microarrays.

responders exhibited densely clustered $CD4^+$ and $CD8^+$ T cells at the TC and periphery, consistent with a "hot" immune phenotype. In contrast, non-responders displayed sparse, diffusely distributed T cells, indicative of an immune-"cold" environment.[40]

In bladder cancer, response to Bacillus Calmette-Guerin therapy correlated with increased baseline infiltration of $CD8^+$ programmed cell death protein 1 $(PD\text{-}1)^+$ T cells and post-treatment elevation of non-regulatory T cells $CD4^+$ Forkhead box P3$(FOXP3)^-$ T cells and active $CD8^+PD\text{-}1^-$ T cells.[42] This finding aligns with a previous study identifying $PD\text{-}1^+CD8^+$ T cells as a subset of tumor-reactive $CD8^+$ T cells with tumor specificity.[77,78] In contrast, Bacillus Calmette-Guerin therapy resistance was linked to higher densities of exhausted $CD8^+PD\text{-}1^+$ T cells in post-treatment tissues.[42] Similar trends were observed in non-small cell lung cancer (NSCLC) patients: responders to neoadjuvant immunochemotherapy exhibited higher density of $CD8^+$, programmed death-ligand 1 $(PD\text{-}L1)^+$, and $CD8^+PD\text{-}L1^+$ cells in the tumor nest, and lower density of $CD3^+FOXP3^+$, $FOXP3^+$, and $CD163^+$ cells.[43]

2.2. T cell-tumor cell spatial proximity

The spatial relationship between T cells and tumor cells is an important determinant of therapeutic efficacy (Figure 2A). IMC analyses in melanoma demonstrated that closer proximity between $CD8^+$ T cells and tumor cells was strongly associated with better responses to ICIs, such as ipilimumab, nivolumab, and pembrolizumab.[54] A high abundance of antigen-experienced T cells in the

Table 1. Cell communities affecting immunotherapy

Tumor	Technology	Cell community	Therapy response	References
TNBC	mIF	High density of $CD8^+$ T cell infiltration before treatment; $CD8^+$ T cells are located farther from $CD15^+$ neutrophils after treatment	Response	38
	IMC	$CD8^+GZMB^+$ T cells interact with tumor cells	Response	39
ESCC	mIF	Denser clusters of $CD4^+$ and $CD8^+$ T cells are observed	Response	40
	IMC	$CD8^+$ T and B cells are increased in TLS regions	Response	41
BCa	mIF	High post-treatment densities of non-Treg $CD4^+FOXP3^-$ T cells and active $CD8^+PD\text{-}1^-$ T cells	Response	42
		High density of exhausted $CD8^+PD\text{-}1^+$ T cells after treatment	Non-response	
NSCLC	mIF	High densities of $CD8^+$, $PD\text{-}L1^+$, and $CD8^+PD\text{-}L1^+$ cells	Response	43
	mIF/WES	$GZMB^+$ CTLs are located close to tumor cells and exhibit higher density	Response	44
	ST	Treg cells are positioned near $Ki67^+$ tumor cells	Non-response	45,46
	ST	Tumor cells are located farther from $CD163^+$ TAMs	Response	47
	mIHC/DSP	$CD68^+$ macrophages interact with $PD1^+$ $FOXP3^+$ Treg cells	Non-response	48
	mIF	M2-polarized TAMs interact with T cells	Non-response	49
	mIHC	High baseline LCAM score	Response	50
	mIHC	Inflamed immunophenotype is present	Response	51
	ST	$CD14^+APOE^+$ cells are colocalized with $MMP7^+$ tumor cells	Non-response	52
	mIF	High proportion of $CD20^+$ B cells within TLS regions	Response	43,53
Melanoma	CyTOF IMC	Decreased distance between melanoma cells and their nearest CTLs	Response	54
	mIHC	Tumor cells interact with $PD\text{-}1^+CD8^+$ T cells	Response	55
	mIHC	Macrophages and T cells interact at the TSI via the PD-1/PD-L1 axis	Non-response	56
	mIF	Lower CTL-to-macrophage ratio and shorter intercellular distances	Non-response	57
	DSP	CD3 and CD8 are expressed within $CD68^+$ macrophage compartments	Response	58
HCC	IMC	$CD8^+$ T cells are in close proximity to Arg1hi+macrophages; MCC and LCC show strong communication with tumor cell communities	Non-response	59
		Physical contact is observed between MCC and LCC	Response	
	ST	Pericancerous macrophages interact with $CD103^+$CTLs	Non-response	60
	IMC	Exhaustion of Kupffer cells enhances the activity of nearby T cells	Response	61
		$CD8^+$ T cells are found close to macrophages	Non-response	
	ST	$POSTN^+$ CAFs colocalized with $PLVAP^+$ endothelial cells, $FOLR2^+$ TAMs, and Tregs	Non-response	62-64
	mIHC	$POSTN^+$ CAFs interact with $CD8^+$ T cells and with $SPP1^+$ macrophages	Non-response	65
	mIHC	$SPP1^+$ macrophages interact with CAFs to promote TIB formation	Non-response	66
HNC	DSP	$CD8^+$ memory T cells show high binding density with Tregs, $CD4^+$ memory T cells, M2 macrophages, cancer cells, and stromal cells	Response	45
	mIF	High spatial relationship	Response	67
		$CD8^+$ T cells are found close to B cells	Non-response	

(*Cont'd...*)

Table 1. (*Continued*)

Tumor	Technology	Cell community	Therapy response	References
MCC	ST	T cells are colocalized with B cells and dendritic cells.	Response	68
ccRCC	ST/mIF	Mesenchymal ccRCC are located near myCAFs at normal adjacent tissues	Non-response	69-71
SCC	ST	"Cold" immune regions are identified	Non-response	72
Pan-cancer	ST	Endothelial cells are enriched near mCAFs; iCAFs are colocalized with $CD8^+$ T cells and interact with immune cells	Non-response	73

Abbreviations: BCa: Bladder cancer; CAF: Cancer-associated fibroblast; ccRCC: Clear cell renal cell carcinoma; CD: Cluster of differentiation; CTL: Cytotoxic T lymphocyte; CyTOF: Cytometry by time of flight; DC: Dendritic cell; DSP: Digital spatial profiling; ESCC: Esophageal squamous cell carcinoma; FOLR2: Folate receptor beta; FOXP3: Forkhead box P3; GZMB: Granzyme B; HCC: Hepatocellular carcinoma; HNC: Head and neck cancer; iCAF: Inflammatory cancer-associated fibroblast; IMC: Imaging mass cytometry; Ki67: Antigen Kiel 67; LCAM: Lung cancer activation module; LCC: Lymphocyte-enriched community; MCC: Macrophage-enriched community; mCAF: Myofibroblastic cancer-associated fibroblast; mIHC: Multiplex immunohistochemistry; mIF: Multiplex immunofluorescence; MMP7: Matrix metallopeptidase 7; NSCLC: Non-small cell lung cancer; PD-1: Programmed cell death protein 1; PD-L1: Programmed death-ligand 1; PLVAP: Plasmalemma vesicle-associated protein; POSTN: Periostin; SCC: Squamous cell carcinoma; SPP1: Osteopontin; ST: Spatial transcriptomics; TAM: Tumor-associated macrophage; TIB: Tumor-immune barrier; TLS: Tertiary lymphoid structure; TNBC: Triple-negative breast cancer; Treg: Regulatory T cell; WES: Whole exome sequencing; TSI: Tumor-stroma interface.

melanoma microenvironment facilitated clustering and repeated contact, enhancing tumor-killing efficiency.[79,80] The spatial proximity and continuous physical interaction between tumor cells and $CD8^+$ T cells contribute to the sustained activation of immune checkpoints and maintenance of immune suppression. For instance, in the pre-treatment melanoma microenvironment, interactions between tumor cells and $PD\text{-}1^+CD8^+$ T cells are strongly associated with the superior efficacy of anti-PD-1 therapy using pembrolizumab.[55,74]

Similarly, IMC analysis in TNBC revealed that baseline interactions between $CD8^+$ Granzyme B $(GZMB)^+$ T cells and cancer cells were the most predictive feature for anti-PD-L1 therapy (atezolizumab) response.[39] In metastatic squamous NSCLC, nearest neighbor analysis revealed that tumors with higher densities of $GZMB^+$ cytotoxic T lymphocytes (CTLs) in close proximity to malignant cells exhibited better responses to nivolumab monotherapy or combination therapy with nivolumab and ipilimumab.[44] These findings reinforce the critical role of cell distribution, particularly CTLs, in determining the efficacy of ICI, consistent with results from other NSCLC studies.[81] Clustering analyses further demonstrated that CTLs and malignant cells aggregated more frequently in responders compared to early progressors, suggesting the presence of a pre-formed antitumor response that is amplified by ICI therapy.[44]

In addition, poor responses to immunotherapy have been linked to the proximity of regulatory T (Treg) cells to antigen Kiel 67-expressing tumor cells. The spatial distribution of Treg cells within the TME and their interactions with specific tumor phenotypes can modulate Treg cell function, ultimately influencing patient outcomes in response to immunotherapy.[45,46]

2.3. T cell-macrophage interactions

Macrophages are a predominant immune cell population in the TME and play a significant role in modulating the effectiveness of immunotherapy by regulating immunosuppressive signals (Figure 2A and B). ST studies in NSCLC have revealed that enrichment of tumor-associated macrophages (TAMs) in the tumor compartment is associated with resistance to immunotherapy, underscoring the importance of their spatial distribution in modulating responses to anti-PD-1/PD-L1 therapies. Notably, patients whose tumor cells were farther from $CD163^+$ TAMs exhibited improved treatment outcomes.[47]

In primary melanoma, a spatially restricted immunosuppressive niche was identified at the tumor-stroma interface (TSI), where interactions between macrophages and T cells are driven by the PD-1/PD-L1 axis.[82] PD-L1 expression was elevated on both M1-like and M2-like macrophages in the TSI among patients who responded to ICIs. However, PD-L1 expression was downregulated in the tumor region but increased again in regions close to CTLs. In these areas, T cells exhibited reduced activation marker expression in proximity to $PD\text{-}L1^+$ macrophages, suggesting that T cell function is regulated in a spatially dependent manner, thereby influencing the efficacy of nivolumab or pembrolizumab.[56] Additional studies have shown that a lower CTL/macrophage ratio and closer proximity between CTLs and macrophages are associated with poorer prognosis.[57]

In NSCLC, the interaction between $CD68^+$ macrophages and $PD1^+FOXP3^+$ Treg cells is preferentially enriched in ICI-refractory tumors, regardless of cell frequency.[48] In hepatocellular carcinoma (HCC), a neoadjuvant trial

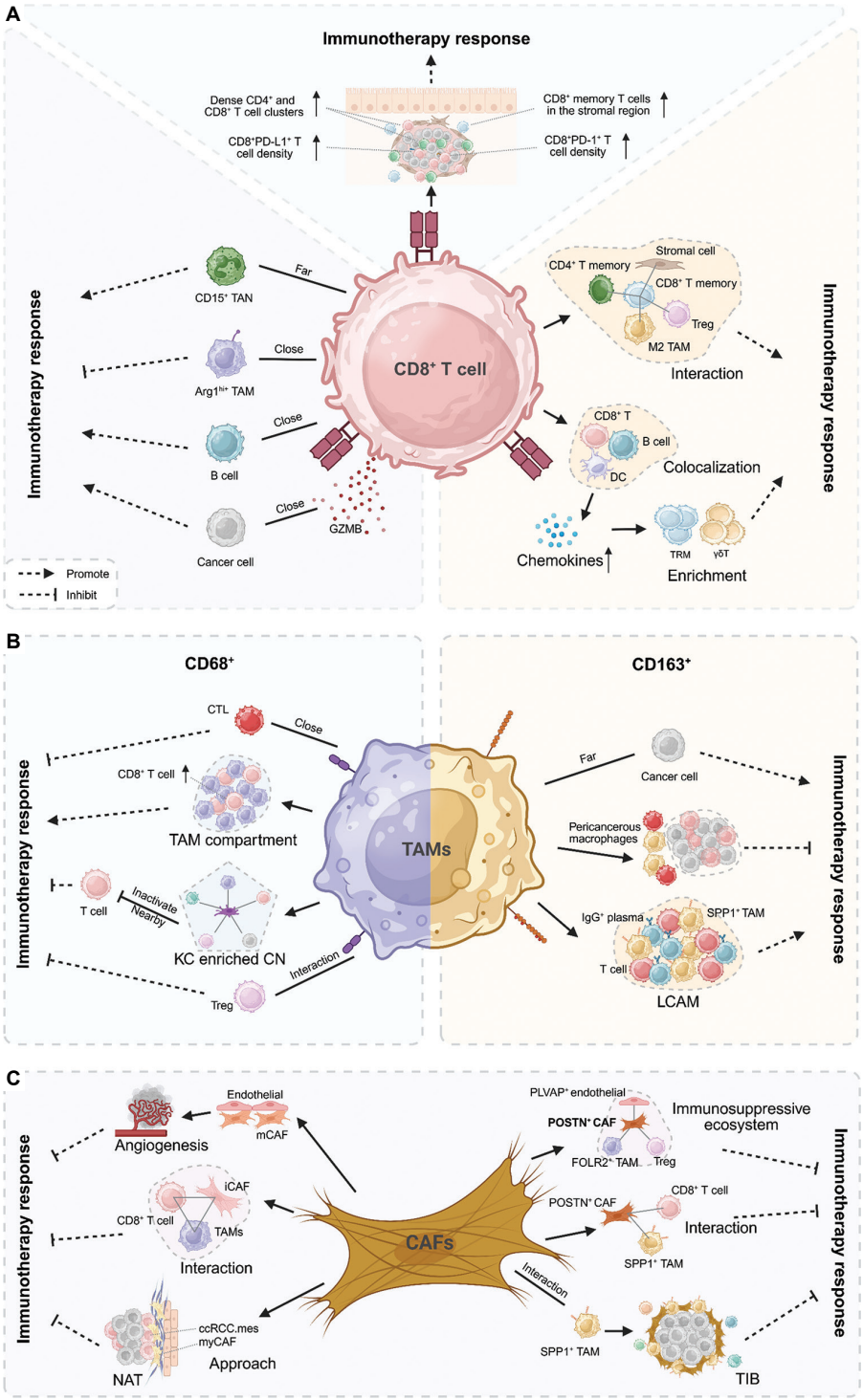

Figure 2. Spatial structures formed by CD8+ T cells, TAMs, and CAFs influence immunotherapy response. (A) The density of CD8+ T cells, their spatial proximity to neighboring cells, and their intercellular interactions collectively modulate the response to immunotherapy; (B) the spatial arrangement of CD68+ M1 and CD163+ M2 macrophages influences immunotherapeutic efficacy; and (C) the architectural organization and extracellular matrix barrier established by cancer-associated fibroblasts impact immunotherapy outcomes. Created using Biorender.com. Shan, J. (2025) https://BioRender.com/p4cme7r.

Abbreviations: CAF: Cancer-associated fibroblast; ccRCC.mes: Mesenchymal clear cell renal cell carcinoma; CD: Cluster of differentiation; CN: Cellular neighborhood; DC: Dendritic cell; FOLR2: Folate receptor beta; GZMB: Granzyme B; IgG: Immunoglobulin G; iCAF: Inflammatory cancer-associated fibroblast; KC: Kupffer cell; LCAM: Local context attention module; mCAF: Myofibroblastic cancer-associated fibroblast; myCAF: Myofibroblastic cancer-associated fibroblast; NAT: Normal adjacent tissue; PLVAP: Plasmalemma vesicle-associated protein; POSTN: Periostin; SPP1: Osteopontin; TAM: Tumor-associated macrophage; TAN: Tumor-associated neutrophil; TIB: Tumor-infiltrating B cell; TRM: Tissue-resident memory T cell; Treg: Regulatory T cell.

combining nivolumab and the tyrosine kinase inhibitor cabozantinib demonstrated that non-responders exhibited closer spatial proximity between CD8+ T cells and macrophages.[83]

Macrophages can further impair immunotherapy by physically blocking T cell contact with tumor cells or by inhibiting communication between T cells and tumor cells. In HCC, IMC profiling identified close proximity of CD8+ T cells to macrophages with high arginase 1 expression, rather than to CD4+ T cells, as a prominent feature of non-responders to cabozantinib-nivolumab combination therapy. In addition, macrophage-enriched communities and lymphocyte-enriched communities in non-responders showed intense communication with tumor cell communities, whereas such interactions were disrupted by contact between macrophage-enriched communities and lymphocyte-enriched communities in responders.[59] Similar mechanisms were reported in lung squamous cell carcinoma, where M2 TAMs prevent T cells from migrating into tumor islets, serving as a key mechanism of resistance to anti-PD-1 immunotherapy.[49] Moreover, cross-presenting peritumoral macrophages failed to eradicate malignant cells and retained CD103+ tumor-reactive CTLs in the peritumoral region in HCC.[60]

However, higher CD3 and CD8 expression levels in the CD68+ compartment were associated with better responses to neoadjuvant nivolumab or combination therapy with nivolumab and ipilimumab in melanoma,[58] suggesting that macrophages can also contribute to enhanced immunotherapy responses. In HCC, Kupffer cell depletion in mouse livers significantly enhanced nearby T cell responses, reduced tumor growth, and sensitized tumors to anti-PD-1 therapy.[61] Overall, the interaction between macrophages and T cells in the TME is complex and context-dependent. The spatial distribution of these cells is crucial in determining the success of immunotherapies. Understanding these interactions offers important insights into predicting and improving immunotherapy efficacy across different cancer types.

2.4. TLS

TLS are increasingly recognized as critical immune structures in the TME, influencing the response to immunotherapy. TLS are organized aggregates of immune cells that form in non-lymphoid tissues and resemble the architecture of secondary lymphoid organs (SLOs). First described by Aloisi and Pujol-Borrell and Drayton *et al.* in 2006,[84,85] TLS typically feature an internal region of CD20+ B cells surrounded by CD3+ T cells, similar to lymphoid follicles in SLOs.[86] While the composition of TLS may vary across different tumor types, follicular helper T cells are generally the dominant T cell subset in the T cell compartment,[87] although CD8+ cytotoxic T cells, helper T cells, and Treg cells may also be present.[88-90] In addition to B and T cells, TLS contain various dendritic cell (DC) subsets, such as CD21+ follicular DCs, which are mesenchymal in origin and are critical for memory B cell selection during the germinal center reaction in SLOs, or CD83+ mature DCs, predominantly located in the T cell zone.[91,92] Furthermore, scattered CD68+ macrophages are present in the follicles to clear apoptotic cells, similar to their function in SLOs.[93] A dense stromal network, similar to the fibroblastic reticular cells in SLOs, anchors TLS within chronically inflamed tissue sites.[94] Specialized vascular structures, such as peripheral node addressin-positive high endothelial venules, mediate the recruitment of lymphocytes.[91]

The formation of TLS is often associated with chronic inflammation, autoimmune diseases, and cancer. In the TME, TLS can facilitate the influx of immune cells into tumor sites through the intratumoral immune cycle.[95,96] The content of TLS varies across tumors, and the presence of mature TLS, high B cell and plasma cell abundance, along with tumor-associated antigen antibodies, generally correlates with favorable clinical outcomes and improved responses to immunotherapy.[97] Consequently, TLS have emerged as a potential biomarkers for predicting therapeutic efficacy.

Spatial analyses of TLS across various tumor types highlight their crucial immune-regulatory role. For example, Kang *et al.*[98] used ST to systematically analyze over 1,000 tumors from 30 cancer types. The study demonstrated that the spatial relationships between TLS components are linked to favorable immunotherapy responses and pathologically defined TLS, suggesting that TLS may serve as a predictive marker for therapeutic efficacy.

The composition of TLS is highly correlated with responses to ICI treatments (Figure 3). For instance, IMC analysis provided a detailed regional evaluation in esophageal squamous cell carcinoma, showing that increases in CD8+ T cells and B cells within TLS following toripalimab treatment were predominantly observed in patients with favorable responses.[41] In NSCLC, mIF analysis demonstrated that patients with a greater number of TLS and a higher proportion of CD20+ B cells within TLS exhibited better responses to anti-PD-1 blockade therapies combined with anlotinib.[43,53]

In melanoma, TLS are considered critical components of the immune microenvironment. DSP analysis revealed that the coexistence of tumor-associated CD8+ T cells and CD20+ B cells in TLS was associated with improved

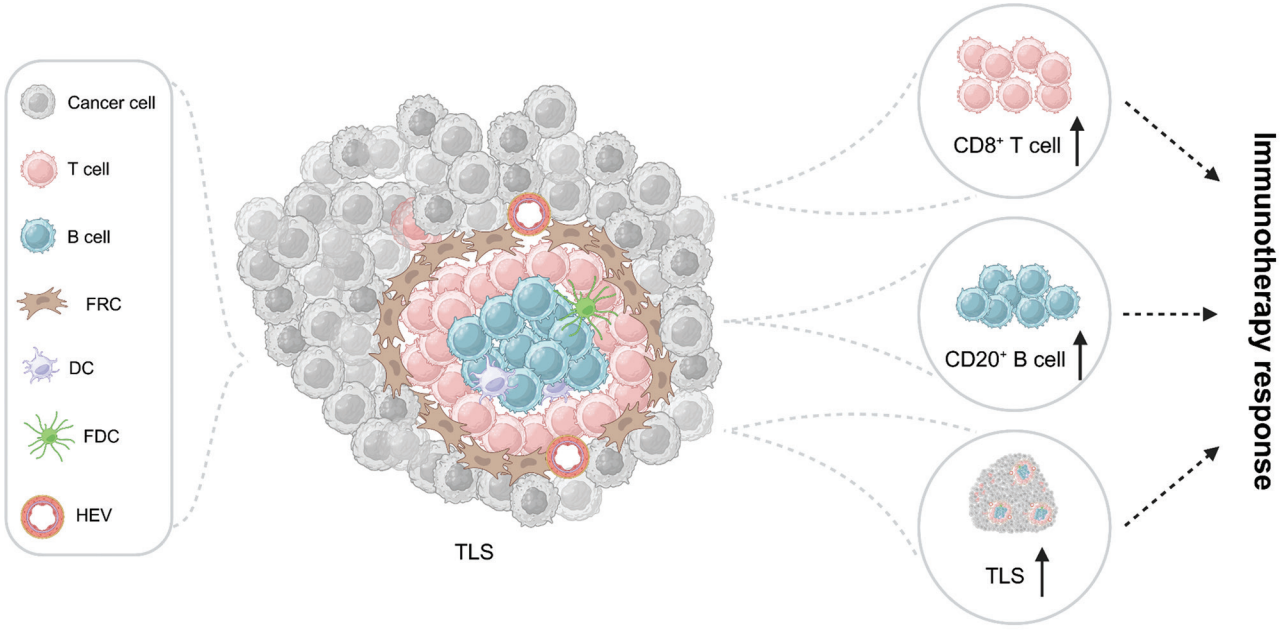

Figure 3. Tertiary lymphoid structure composition associated with immune checkpoint inhibitor response. The cellular composition of the tertiary lymphoid structure is strongly associated with the response to immune checkpoint inhibitor therapy. Patients exhibiting favorable outcomes typically show abundant TLS formation, characterized by increased infiltration of $CD20^+$ B cells and $CD8^+$ T cells within the TLS. The figure was created using Biorender.com. Shan, J. (2025) https://BioRender.com/7z7qbwf.
Abbreviations: CD: Cluster of differentiation; DC: Dendritic cell; FDC: Follicular dendritic cell; FRC: Fibroblastic reticular cell; HEV: High endothelial venule; TLS: Tertiary lymphoid structure.

responses to ipilimumab therapy and prolonged survival.[17] Furthermore, ST-based B cell analysis demonstrated clonal diversification, selection, and expansion within TLS, as well as the presence of fully mature clonotypes at distant sites in tumors containing TLS. Tumors with TLS exhibited a high frequency of immunoglobulin G (IgG)-producing plasma cells, along with IgG staining and apoptotic malignant cells, suggesting a response to nivolumab and ipilimumab.[99]

In colorectal cancer (CRC), studies showed that the TLS gene signature was significantly associated with immunotherapy response. mIF results confirmed that high expression of the paired related homeobox 1 (*PRRX1*) gene and its transcript, *PRRX1*-mRNA, in TLS enhanced local T cell and B cell activity, promoting immune responses in the TME.[100] These findings highlight the important role of TLS in the TME, promoting immune activation and modulating immune suppression. Therapeutic strategies to induce TLS formation should be explored to improve responses to cancer immunotherapy.

2.5. Other immune spatial modules

T cells form complex networks of interaction with other immune cells. One study identified a lung cancer activation module in NSCLC, consisting of $PDCD1^+CXCL13^+$ activated T cells, IgG^+ plasma cells, and osteopontin $(SPP1)^+$ macrophages. Elevated baseline scores for this activation module were associated with improved responses to atezolizumab immunotherapy.[50] In head and neck cancer, DSP and spatial proteomics analyses showed that the stromal compartment of immunotherapy-responsive patients contained higher densities of $CD8^+$ memory cells. In patients responding to pembrolizumab or nivolumab, $CD8^+$ memory cells were found at greater densities in spatial proximity to macrophages, Treg cells, $CD4^+$ memory cells, M2 macrophages, cancer cells, and stromal cells.[45]

Using ST technology, researchers observed frequent colocalization of T cells, B cells, and DCs in Merkel cell carcinoma tumors, where these immune subsets provided chemokines and co-stimulatory signals. This spatial arrangement significantly enhanced the clonal expansion or recruitment of tissue-resident memory (TRM) T cells and Vδ1 γδT cells, leading to improved responses to immunotherapy.[68] Similarly, research by Gil-Jimenez *et al.*[67] reported that the spatial relationship between $CD8^+$ T cells or macrophages and adjacent cancer cells—quantified by approximating the first-nearest-neighbor distance distribution using a Weibull distribution—was positively associated with response to ipilimumab-nivolumab

combination therapy. In contrast, closer proximity between CD8⁺ T cells to B cells was characteristic of non-responders.

In addition, artificial intelligence-supported multiplex immunohistochemistry (mIHC) analyses revealed that specific infiltration patterns can predict responses to ICI therapy in NSCLC. Patients with inflammatory immune phenotypes demonstrated better responses to pembrolizumab, nivolumab, and atezolizumab compared to those with immune-exclusion or immune-desert phenotypes.[51] Furthermore, ST analyses in NSCLC revealed that a higher degree of colocalization between CD14⁺APOE⁺ cells and matrix metallopeptidase 7 (MMP7)⁺ tumor cells was observed in patients with poor responses to immunotherapy. This spatial configuration was associated with reduced T cell infiltration and impaired TLS formation.[52]

2.6. Cancer-associated fibroblasts and immune exclusion

The distribution of cancer-associated fibroblasts (CAFs) and their interactions with other cell types in the TME directly affect immunotherapy outcomes (Figure 2C). In multiple cancer types, CAFs regulate the ECM, altering physical characteristics, such as tumor stiffness and density, and forming an immune barrier that obstructs therapeutic drugs and immune cells from penetrating the tumor, thereby reducing therapeutic efficacy.[101] A pan-cancer study based on ST showed that, compared to other cell types, inflammatory CAFs (iCAFs), matrix CAFs (mCAFs), metabolic CAFs, and proliferative CAFs display higher spatial proximity to one another. Notably, endothelial cells were enriched near mCAFs, and their intercellular communication promoted angiogenesis in the TME. Furthermore, iCAFs were frequently colocalized with CD8⁺ T cells in several tumor types. The interactions between iCAFs and immune cells, particularly macrophages and CD8⁺ T cells, contributed to the establishment of an immunosuppressive microenvironment, resulting in poor responses to pembrolizumab immunotherapy.[73]

In clear cell renal cell carcinoma (ccRCC), ST and mIF analyses revealed that myofibroblastic CAFs form fibrotic structures visible at the tumor-normal adjacent tissue interface, sometimes intruding into normal tissue. Mesenchymal-like ccRCC cells preferentially localize in these regions. Their spatial proximity at the tumor-normal adjacent tissue interface, forming an immune-exclusion barrier, is a key feature of microenvironments associated with poor prognosis and resistance to ipilimumab or nivolumab.[69-71]

Periostin (POSTN)⁺ CAFs predominantly appear in peripheral tumor regions and play a leading role in ECM remodeling. This remodeling forms a physical barrier that impedes the recruitment of immune cells, particularly T cells, into tumor sites.[102,103] In HCC, ST analyses confirmed that POSTN⁺ CAFs colocalize with immunosuppressive plasmalemma vesicle-associated protein (PLVAP)⁺ endothelial cells, folate receptor beta (FOLR2)-positive TAMs, and Treg cells to form an immunosuppressive ecosystem. POSTN⁺ CAFs were identified as the central hub of interactions in the HCC onco-fetal niche.[62-64] Another study clarified the interactions between POSTN⁺ CAFs and CD8⁺ T cells, as well as between POSTN⁺ CAFs and SPP1⁺ macrophages, forming an immunosuppressive microenvironment that limits the response to tocilizumab immunotherapy.[65] Furthermore, SPP1⁺ macrophages have been shown to interact with CAFs, stimulating ECM remodeling and promoting the formation of tumor immune barrier structures, which restrict immune infiltration into the TC. Blocking SPP1, or macrophage-specific knockout of SPP1, significantly enhanced the efficacy of anti-PD-1 therapy in mouse liver cancer.[66] The critical role of CAFs in shaping the TME underscores the need for in-depth research to develop therapies targeting specific CAFs subtypes.

In addition, intratumoral heterogeneity has a profound impact on directing the spatial organization and function of tumor-infiltrating immune cells, resulting in the formation of "cold" immune regions characterized by insufficient T cell infiltration, thereby reducing the efficacy of PD-1 inhibitors.[72] These factors determine immunotherapy response by altering the location, activity, and function of immune cells. A deeper understanding of these interactions can provide new ideas for optimizing immunotherapy strategies and improving patient survival rates.

3. Spatial architecture shaping radiotherapy efficacy

Radiotherapy eliminates cancer cells by inducing lethal DNA breaks through high-energy ionizing radiation. Over 50% of cancer patients undergo radiotherapy during treatment.[104] However, dose escalation—often necessary for effective tumor control—increases the risk of damage on healthy tissues surrounding the irradiated area. Therefore, advanced radiotherapy modalities, such as intensity-modulated radiation therapy, helical tomotherapy, and proton therapy have been developed to address these challenges.[105] Although these technologies can alleviate radiation-induced toxicity to some extent, the benefit remains relatively limited.[106] As such, achieving safer and more precise radiotherapy delivery continues to be a primary goal in radiation oncology.

3.1. Immune cell distribution

Recent research has increasingly focused on the spatial structure of tumor boundaries in the TME, highlighting their predictive role in radiotherapy response. The spatial distribution of infiltrating immune and stromal cells significantly affects tumor sensitivity to radiotherapy. In locally advanced rectal cancer (LARC), IMC revealed that the spatial distribution of tumor-infiltrating $CD8^+$ T cells and TAMs is closely associated with the response to neoadjuvant chemoradiotherapy (nCRT). Responders exhibited higher densities of $CD8^+$ T cells, whereas non-responders displayed elevated densities of TAMs and Treg cells.[107] Similarly, another study in CRC revealed that a high density of M2 macrophages strongly predicted poorer nCRT response.[108] In LARC, a combined DSP and mIF analysis revealed that high expression of immune markers, such as human leukocyte antigen-DR isotype/major histocompatibility complex class II, and a high density of $CD20^+$ B cells in the stroma, were associated with better response to nCRT.[109] In brain tumors, highly multiplexed immunofluorescence imaging demonstrated extensive spatial reorganization of immune cell populations and structures following radiotherapy.[21]

3.2. Stromal components

In addition to immune cell infiltration, the stromal components of the TME significantly affect radiotherapy response. Research shows that vimentin expression and the tumor-stroma ratio (TSR) in tumor tissues are important indicators for predicting nCRT efficacy. IMC analysis in LARC patients revealed that reduced vimentin expression and an elevated TSR were associated with better responses to nCRT. Multivariate analyses further identified the combination of vimentin and TSR as an independent predictor of nCRT response.[110] Similarly, the tumor-stroma contact ratio (TSC) is also a critical predictor of radiochemotherapy response in locally advanced oropharyngeal squamous cell carcinoma. Higher TSC has been correlated with poorer radiotherapy response and shorter survival.[111]

In summary, the distribution patterns of immune and stromal cells have a crucial impact on radiotherapy response. The infiltration level and activity of immune cells, the spatial distribution of stromal cells, and the complex interactions at the tumor margin collectively determine radiotherapy efficacy (Table 2). A deeper understanding of these spatial dynamics and their relationship with radiotherapy response provides critical insights for developing optimized and personalized radiotherapy strategies, ultimately improving patient outcomes.

Table 2. Cell communities affecting radiotherapy

Tumor	Technology	Cell community	Therapy response	References
LARC	IMC	Higher density of $CD8^+$ T cells	Response	107
		Higher density of TAMs and Tregs	Non-response	
	mIF/DSP	High density of $CD20^+$ B cells in the stroma	Response	109
	IMC	Increased TSR	Non-response	110
OPSCC	mIF	Higher TSC	Non-response	111

Abbreviations: CD: Cluster of differentiation; DSP: Digital spatial profiling; IMC: Imaging mass cytometry; LARC: Locally advanced rectal cancer; mIF: Multiplex immunofluorescence; OPSCC: Oropharyngeal squamous cell carcinoma; TAM: Tumor-associated macrophage; Treg: Regulatory T cell; TSC: Tumor-stroma contact ratio; TSR: Tumor-stroma ratio.

4. Spatial regulation of chemotherapy outcomes

Conventional chemotherapy is the most common treatment for solid tumors, with specific regimens varying by tumor type and stage. However, the therapeutic benefits of cytotoxic drugs vary significantly among patients.[112] A major challenge lies in understanding and predicting which patients are unlikely to benefit from such regimens, as this can affect treatment decisions and quality of life.[113] Multiple studies indicate that interactions among immune cells, fibroblasts, stromal components, and vasculature in the TME directly influence chemotherapy efficacy and patient prognosis (Table 3). Notably, the spatial distribution and functional states of immune cells are critical regulators of chemotherapy response.

4.1. Immune structures and chemosensitivity

In TNBC, DSP revealed that increased estrogen receptor-α expression and reduced 4-1BB and melanoma antigen recognized by T cells 1 in the stromal compartment were associated with responses to adjuvant chemotherapy with 5-fluorouracil, epirubicin, and cyclophosphamide, while higher expression of granzyme A, stimulator of interferon genes, and fibronectin, along with lower CD80 levels in the tumor compartment, were linked to therapy response.[114] In a study on intrahepatic cholangiocarcinoma, patients with rapid progress (RP; survival <6 months) or long survival (LS; survival >23 months) were examined. Using mIF, it was found that tumor-intrinsic processes, tumor-myeloid interactions, and tumor-T cell interactions contributed to RP/LS-associated platinum-combination chemotherapy resistance.[115] The reduced sensitivity of RP-like cell lines

Table 3. Cell communities affecting chemotherapy

Tumor	Technology	Cell community	Therapy response	References
TNBC	DSP	Increased estrogen receptor-α expression and reduced 4-1BB and MART1 in the stromal compartment	Response	114
		Higher expression of GZMA, STING, and fibronectin, and lower expression of CD80 in the tumor compartment	Non-response	
iCCA	mIF	Tumor-myeloid interactions; tumor-T cell interactions	Non-response	115
NSCLC	mIF	Dens; InS; TrPS; CMV	Response	116
	mIF	TRM cells showed increased density, infiltration scores, and proximity to cancer cells	Response	117
Gastric cancer	mIF	Higher Treg and $CD163^+$ M2-like macrophage density before NAC; higher $CD8^+$: $CD4^+$ ratios and $CD86^+$ M1: CD163+ M2-like macrophage ratios after NAC; notable colocalization between tumors and $CD163^+$ M2-like macrophages	Response	118,119
CRC	mIHC	CCIM	Non-response	120
LARC	IMC	Increased TSR	Non-response	110
OPSCC	mIF	Higher TSC	Non-response	111
PDAC	ST/DSP	myCAFs adjacent to cancer cells; iCAFs colocalized with NRP and BSL/MES cancer cells; NRP cancer cells colocalized with CD8+ T cells	Non-response	121,122

Abbreviations: BSL: Basal-like; CCIM: Colorectal cancer immune module; CD: Cluster of differentiation; CMV: Cancer microvasculature; CRC: Colorectal cancer; DSP: Digital spatial profiling; GZMA: Granzyme A; iCAF: Inflammatory cancer-associated fibroblast; iCCA: Intrahepatic cholangiocarcinoma; IMC: Imaging mass cytometry; InS: Infiltration score; LARC: Locally advanced rectal cancer; MART1: Melanoma antigen recognized by T cells 1; MES: Mesenchymal; mIHC: Multiplex immunohistochemistry; mIF: Multiplex immunofluorescence; myCAF: Myofibroblastic cancer-associated fibroblast; NAC: Neoadjuvant chemotherapy; NRP: Neural-like progenitor; NSCLC: Non-small cell lung cancer; OPSCC: Oropharyngeal squamous cell carcinoma; PDAC: Pancreatic ductal adenocarcinoma; ST: Spatial transcriptomics; STING: Stimulator of interferon genes; TAM: Tumor-associated macrophage; TNBC: Triple-negative breast cancer; TRM: Tissue-resident memory T cell; TrPS: Tumor proximity score; Treg: Regulatory T cell; TSC: Tumor-stroma contact ratio; TSR: Tumor-stroma ratio.

could result from metabolic reprogramming, such as increased glycolysis, which has been shown to confer chemoresistance to cytotoxic drugs in multiple cancers.[123,124]

In immunosuppressive microenvironments, macrophages can metabolically inactivate gemcitabine before its uptake by cancer cells and shorten mitotic arrest duration following DNA damage, limiting the antitumor effects of chemotherapy. Furthermore, myeloid cells co-present tumor antigens with immunosuppressive molecules, promoting Treg expansion and tumor tolerance, ultimately creating a stable, immune-inert state.

In neoadjuvant chemotherapy (NAC) studies of NSCLC, mIF analyses showed that Treg cell density, infiltration score, and Treg-$CD8^+$ T cell proximity score were significantly associated with better chemotherapy response.[116] Another NSCLC study demonstrated that TRM increased in density, infiltration, and proximity to cancer cells following NAC. These changes were associated with improved response and prognosis under regimens, such as platinum combined with taxane, pemetrexed, or gemcitabine.[117]

In locally advanced gastric cancer, mIF analysis revealed that pre-NAC Treg and $CD163^+$ M2-like macrophage densities were significantly higher in responders than in non-responders. Following NAC with the FLOT regimen (docetaxel, oxaliplatin, fluorouracil, and leucovorin), responders exhibited elevated $CD8^+/CD4^+$ T cell ratios and $CD86^+$ M1/$CD163^+$ M2-like macrophage ratios compared to non-responders. Spatial assessments further demonstrated enhanced colocalization of tumor cells and $CD163^+$ M2-like macrophages in responders.[118,119] In CRC, mIHC analysis identified a CRC immune module comprising $FOLR2^+$ macrophages, Treg cells, exhausted $CD4^+$ and $CD8^+$ T cells, and tolerant $CD8^+$ T cells, which was predictive of lower chemotherapy sensitivity.[120]

4.2. Stromal barriers and vascular remodeling

Stromal components in the TME also play a critical role in chemotherapy response. Through IMC and mIF analyses, a high stromal proportion was identified as a strong predictor of poor chemotherapy response in LARC and locally advanced oropharyngeal squamous cell carcinoma.[110,111] Stromal cells can form a barrier through ECM remodeling,

hindering chemotherapy drug penetration and resulting in poor chemotherapy outcomes.

In pancreatic ductal adenocarcinoma samples that responded poorly to neoadjuvant therapy, ST analysis revealed that myofibroblastic CAFs tended to be adjacent to cancer cells, while iCAFs were specifically colocalized with neural-like progenitor (NRP) and basal/mesenchymal cancer cells, and NRP cancer cells colocalized with $CD8^+$ T cells. These interactions contributed to resistance to multi-cycle FOLFIRINOX (folinic acid, fluorouracil, irinotecan, and oxaliplatin) treatment.[121] These findings are consistent with the DSP-identified "treatment-enriched community" in pancreatic ductal adenocarcinoma, composed of NRP and mesenchymal cancer cells, iCAFs, and $CD8^+$ T cells.[122]

Vascular remodeling in the TME also plays a pivotal role in modulating chemotherapy outcomes. In NSCLC, Treg-$CD8^+$ and Treg-$CD4^+$ cell proximity scores were negatively correlated with cancer microvasculature and CAF density, indicating a complex interaction between angiogenesis and immunosuppression that influences response to chemotherapy agents, such as gemcitabine, pemetrexed, and taxel.[116] Moreover, after NAC with CAPOX (capecitabine combined with oxaliplatin) or FOLFOX (leucovorin calcium, fluorouracil, and oxaliplatin) regimens, an increase in $CD31^+$ microvasculature density showed a positive correlation with TRM and non-TRM T cells.[118]

Taken together, the cellular composition and spatial organization in the TME exert important regulatory functions in chemotherapy response across tumor types. Immune structures, stromal components, and vascular remodeling collectively influence treatment strategies and outcomes.

5. Spatial regulation of targeted therapy outcomes

Targeted therapy has revolutionized cancer treatment by shifting from cytotoxic chemotherapy to precision therapy. This shift was driven by the identification of malignant "driver" mutations, which promote malignant phenotypes and sustain cancer cell proliferation. Cancer cells often exhibit dependence on these drivers, making their inhibition an effective therapeutic strategy that frequently induces cell death.[125,126] Targeted drugs are classified into two main categories: large-molecule monoclonal antibodies and small-molecule kinase inhibitors.

Although targeted therapy elicits effective responses with lower toxicity, resistance frequently develops in advanced diseases due to factors contributing to intratumoral heterogeneity.[127] Omics-based research aimed at uncovering resistance mechanisms, identifying synergistic drug combinations, and discovering predictive biomarkers underscores the potential for personalized therapy.[128-130]

5.1. Immune cell composition and drug sensitivity

Research has shown that the quantity and spatial distribution of TILs significantly influence the efficacy of human epidermal growth factor receptor 2 (HER2)-targeted therapy (Table 4). In HER2-positive breast and gastric cancers, mIF analysis revealed that favorable responses to lapatinib were significantly associated with higher baseline infiltration of stromal $CD4^+$, intratumoral $CD4^+$, and intratumoral $CD20^+$ TILs.[131,132]

Table 4. Cell communities affecting targeted therapy

Tumor	Technology	Cell community	Therapy response	References
Breast cancer	mIF	Higher baseline stromal $CD4^+$, intratumoral $CD4^+$, and intratumoral $CD20^+$ TIL infiltration	Response	131,132
Gastric cancer	mIHC	Higher interaction scores among NK cells and $CD8^+$ T cells, B cells and M2 macrophages, and B cells and Tregs	Response	133
RCC	IMC	TLS-like CN phenotypes $CD8^+$ T cell-B cell and $GZMB^+CD8^+$ T cell-B cell interactions	Response	134
HCC	ST	Interactions between HCC cells and CAFs	Non-response	135
		Regions of high PD-L1 expression	Response	59
OSCC	ST	LE gene signatures	Non-response	136
		TC gene signatures	Response	

Abbreviations: CAF: Cancer-associated fibroblast; CD: Cluster of differentiation; CN: Cellular neighborhood; GZMB: Granzyme B; HCC: Hepatocellular carcinoma; IMC: Imaging mass cytometry; LE: Leading edge; mIF: Multiplex immunofluorescence; mIHC: Multiplex immunohistochemistry; NK cell: Natural killer cell; OSCC: Oral squamous cell carcinoma; PD-L1: Programmed death-ligand 1; RCC: Renal cell carcinoma; ST: Spatial transcriptomics; TC: Tumor core; TIL: Tumor-infiltrating lymphocyte; TLS: Tertiary lymphoid structure; Treg: Regulatory T cell.

In gastric cancer, mIHC further demonstrated that post-treatment infiltration of natural killer cells, CD8⁺ T cells, and B cells was significantly increased in responders to HER2-targeted therapy. Spatial analyses in these patients revealed higher interaction scores between natural killer cells and CD8⁺ T cells, B cells, and M2 macrophages, and B cells and Treg cells. These interactions effectively inhibited the immunosuppressive activity of M2 macrophages and Treg cells.[133]

In addition, in metastatic melanoma, an integrated analysis of digital pathology and transcriptomics indicated that activated CD8⁺ T cells located in less densely populated regions were closely associated with reduced tumor cell proliferation and improved efficacy of *BRAF* inhibitors,

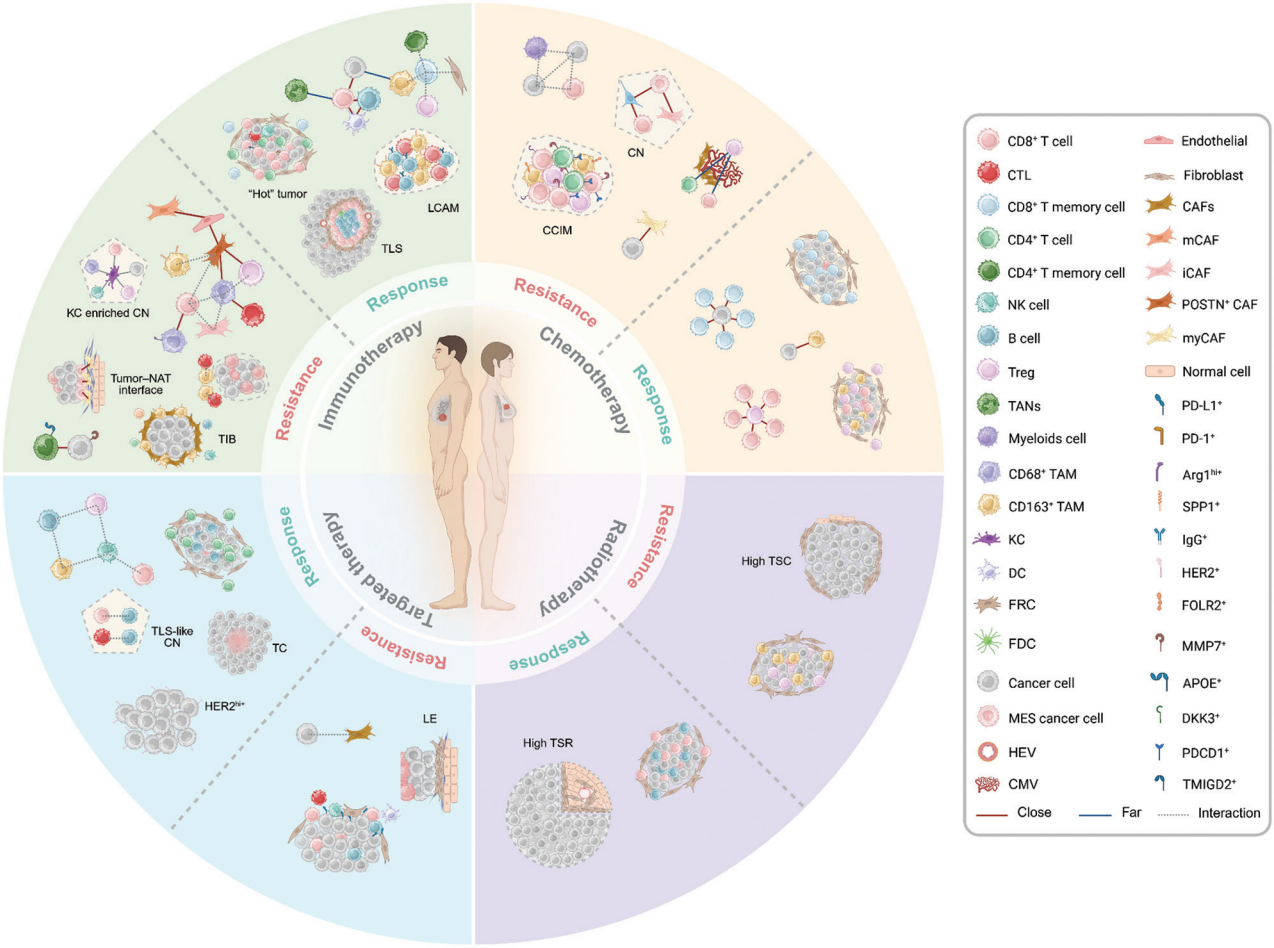

Figure 4. Spatial structures predicting therapeutic response or resistance to immunotherapy, chemotherapy, radiotherapy, or targeted therapy. Different cellular states and types, their spatial proximity or separation within different tumor regions, and their interactions form spatial structures—such as TLS, CN, TIB, LCAM, and the CRC immune module. In addition, TSR, TSC, and the spatial heterogeneity of therapeutic target expression can collectively predict patient response to immunotherapy, chemotherapy, radiotherapy, or targeted therapy. The figure was created using Biorender.com. Shan, J. (2025) https://BioRender.com/x16c605.

Abbreviations: APOE: Apolipoprotein E; Arg1: Arginase 1; CAF: Cancer-associated fibroblast; CCIM: Colorectal cancer immune module; CD: Cluster of differentiation; CMV: Cancer microvasculature; CN: Cellular neighborhood; CRC: Colorectal cancer; CTL: Cytotoxic T lymphocyte; DC: Dendritic cell; DKK3: Dickkopf WNT signaling pathway inhibitor 3; FDC: Follicular dendritic cell; FOLR2: Folate receptor beta; FRC: Fibroblastic reticular cell; HEV: High endothelial venule; HER2: Human epidermal growth factor receptor 2; iCAF: Inflammatory cancer-associated fibroblast; IgG: Immunoglobulin G; KC: Kupffer cell; LCAM: Lung cancer activation module; LE: Leading edge; MES: Mesenchymal; mCAF: Matrix cancer-associated fibroblast; mYCAF: Myofibroblastic cancer-associated fibroblast; MMP7: Matrix metalloproteinase 7; NAT: Normal adjacent tissue; NK: Natural killer; PD-1: Programmed cell death protein 1; PD-L1: Programmed death-ligand 1; PDCD1: Programmed cell death 1; POSTN: Periostin; SPP1: Osteopontin; TIB: Tumor-infiltrating B cell; TAM: Tumor-associated macrophage; TAN: Tumor-associated neutrophil; TC: Tumor core; Treg: Regulatory T cell; TLS: Tertiary lymphoid structure; TMIGD2: Transmembrane and immunoglobulin domain containing 2; TSC: Tumor-stroma contact ratio; TSR: Tumor-stroma ratio.

such as vemurafenib, dabrafenib, dabrafenib-trametinib, and encorafenib-binimetinib.[137]

In ccRCC, IMC-based cell neighborhood analysis subdivided TME phenotypes and identified TLS-like phenotypes with abundant $CD8^+$ T cell-B cell and $GZMB^+CD8^+$ T cell-B cell interactions, which were correlated with improved outcomes and responses to sunitinib treatment.[134]

Stromal components in the TME also influence targeted therapy. In HCC, ST analysis demonstrated that interactions between HCC cells and CAFs remodel the ECM, creating a physical barrier that limits the penetration and efficacy of targeted drugs, such as cabozantinib.[135]

5.2. Spatial heterogeneity of target expression

The spatial heterogeneity of therapeutic target expression also affects the efficacy of targeted therapy (Table 4). Studies have revealed that HER2 expression exhibits intralesional spatial heterogeneity (within a single tumor lesion), interlesional spatial heterogeneity (among different tumor sites), and temporal heterogeneity (during treatment). Spatial and temporal heterogeneity may influence both the response to and resistance against HER2-targeted agents, and their prevalence and predictive roles vary across HER2-overexpressing solid tumors.[138-143] Areas with high HER2 expression often respond better to HER2-targeted therapies—including lapatinib, tucatinib, neratinib, or pyrotinib—while areas with low HER2 expression may escape treatment.[132] Such spatial heterogeneity not only affects initial treatment responses but also contributes to drug resistance.

Research on oral squamous cell carcinoma further revealed a connection between regional gene expression and response to targeted therapy. Using ST, researchers identified structural heterogeneity between the TC and margin. The margin-associated gene expression profile was conserved across multiple cancers and correlated with poorer clinical outcomes. In contrast, the TC signature was tissue-specific and associated with favorable therapeutic responses in multiple cancer types.[136]

In HCC, spatial heterogeneity of PD-L1 expression also influences response to immunotherapy combined with targeted therapy. IMC analyses revealed that PD-L1 levels on tumor cells were significantly higher at the immune-tumor boundary than in more distant regions in non-responders. Regions with high PD-L1 expression demonstrated better responses to ICIs, such as cabozantinib, whereas areas with low PD-L1 expression were more likely to evade immune surveillance.[59] These findings highlight the critical influence of spatially heterogeneous target expression on treatment outcomes and underscore the importance of spatial profiling in optimizing therapeutic strategies.

6. Conclusion

The spatial heterogeneity of the TME has emerged as a critical determinant of therapeutic outcomes across diverse cancer types. While traditional methods have focused on cellular composition and gene expression, recent advances in spatial omics technologies now enable high-resolution mapping of the TME, revealing how the location, interaction, and structural organization of cellular communities influence treatment responses. Importantly, spatial omics technologies have demonstrated that it is not merely cellular composition, but the relative positioning, interaction density, and compartmental organization of these cells that determine therapeutic responses (Figure 4). Future advancements in spatial omics will further drive TME research by constructing comprehensive ecosystem maps and elucidating the mechanisms underlying specific structural modules. The discovery of such spatial architectures will provide new insights into the development of personalized tumor treatment strategies, ultimately advancing precision therapy for individual patients. To achieve these goals, several key scientific questions require further investigation.

Despite its promise, this field remains in its early stages, and many critical questions must still be addressed, including:

(i) Are there other conserved cellular communities, such as TLS, that play essential roles across different tumor types?
(ii) Do cellular communities with distinct compositions undergo dynamic transitions during treatment?
(iii) How do these transitions influence therapeutic outcomes?

These questions necessitate further investigation using spatial omics in combination with lineage-tracing techniques. Moreover, the molecular characteristics of therapy-resistant regions remain incompletely understood. Future research integrating spatial multi-omics analysis may enable a more detailed characterization of the molecular networks within these niches, facilitating the identification of more precise therapeutic targets. Finally, as cell communities represent structured and spatially organized entities, determining how to experimentally validate their function and dynamics *in situ* remains a major challenge.

In conclusion, future research on the structural heterogeneity of the TME must focus not only on refining spatial omics technologies—by enhancing resolution, optimizing analytical workflows, and integrating methodologies—but also on combining these advancements with functional experiments, clinical trials, and multicenter validation. These efforts will be essential

for promoting the broad clinical application of spatial omics in precision oncology.

Acknowledgments

None.

Funding

This work was supported by the National Natural Science Foundation of China (NSFC) (91959206) and the National Key R&D Program of China (2022YFC3401600).

Conflict of interest

The authors declare that they have no competing interests.

Author contributions

Conceptualization: Xuan Cui, Juanjuan Shan, Cheng Qian
Visualization: Xuan Cui, Yuanli Ni, Lan Zhao
Writing – original draft: Xuan Cui, Xia Lei
Writing – review & editing: Juanjuan Shan, Cheng Qian

Ethics approval and consent to participate

Not applicable.

Consent for publication

Not applicable.

Availability of data

Not applicable.

Further disclosure

ChatGPT was employed by the authors to improve the language clarity and readability of this manuscript, and the content was reviewed and appropriately edited afterward. The authors take full responsibility for the content of the publication.

References

1. Bayik D, Lathia JD. Cancer stem cell-immune cell crosstalk in tumour progression. *Nat Rev Cancer*. 2021;21(8):526-536.
   doi: 10.1038/s41568-021-00366-w
2. Fu T, Dai LJ, Wu SY, *et al*. Spatial architecture of the immune microenvironment orchestrates tumor immunity and therapeutic response. *J Hematol Oncol*. 2021;14(1):98.
   doi: 10.1186/s13045-021-01103-4
3. Walsh LA, Quail DF. Decoding the tumor microenvironment with spatial technologies. *Nat Immunol*. 2023;24(12):1982-1993.
   doi: 10.1038/s41590-023-01678-9
4. Jin MZ, Jin WL. The updated landscape of tumor microenvironment and drug repurposing. *Signal Transduct Target Ther*. 2020;5(1):166.
   doi: 10.1038/s41392-020-00280-x
5. Lu MY, Sater HA, Mahmood F. Multiplex computational pathology for treatment response predication. *Cancer Cell*. 2021;39(8):1053-1055.
   doi: 10.1016/j.ccell.2021.07.014
6. Elhanani O, Ben-Uri R, Keren L. Spatial profiling technologies illuminate the tumor microenvironment. *Cancer Cell*. 2023;41(3):404-420.
   doi: 10.1016/j.ccell.2023.01.010
7. Dirkse A, Golebiewska A, Buder T, *et al*. Stem cell-associated heterogeneity in Glioblastoma results from intrinsic tumor plasticity shaped by the microenvironment. *Nat Commun*. 2019;10(1):1787.
   doi: 10.1038/s41467-019-09853-z
8. Sheng W, Zhang C, Mohiuddin TM, *et al*. Multiplex immunofluorescence: A powerful tool in cancer immunotherapy. *Int J Mol Sci*. 2023;24(4):3086.
   doi: 10.3390/ijms24043086
9. Giesen C, Wang HA, Schapiro D, *et al*. Highly multiplexed imaging of tumor tissues with subcellular resolution by mass cytometry. *Nat Methods*. 2014;11(4):417-422.
   doi: 10.1038/nmeth.2869
10. Ståhl PL, Salmén F, Vickovic S, *et al*. Visualization and analysis of gene expression in tissue sections by spatial transcriptomics. *Science*. 2016;353(6294):78-82.
   doi: 10.1126/science.aaf2403
11. Merritt CR, Ong GT, Church SE, *et al*. Multiplex digital spatial profiling of proteins and RNA in fixed tissue. *Nat Biotechnol*. 2020;38(5):586-599.
   doi: 10.1038/s41587-020-0472-9
12. Lin JR, Fallahi-Sichani M, Chen JY, Sorger PK. Cyclic immunofluorescence (CycIF), a highly multiplexed method for single-cell imaging. *Curr Protoc Chem Biol*. 2016;8(4):251-264.
   doi: 10.1002/cpch.14
13. Goltsev Y, Samusik N, Kennedy-Darling J, *et al*. Deep profiling of mouse splenic architecture with CODEX multiplexed imaging. *Cell*. 2018;174(4):968-981.e15.
   doi: 10.1016/j.cell.2018.07.010
14. Radtke AJ, Kandov E, Lowekamp B, *et al*. IBEX: A versatile multiplex optical imaging approach for deep phenotyping and spatial analysis of cells in complex tissues. *Proc Natl Acad Sci U S A*. 2020;117(52):33455-33465.
   doi: 10.1073/pnas.2018488117
15. Keren L, Bosse M, Thompson S, *et al*. MIBI-TOF: A multiplexed imaging platform relates cellular phenotypes

and tissue structure. *Sci Adv*. 2019;5(10):eaax5851.

doi: 10.1126/sciadv.aax5851

16. Mund A, Coscia F, Kriston A, *et al*. Deep visual proteomics defines single-cell identity and heterogeneity. *Nat Biotechnol*. 2022;40(8):1231-1240.

doi: 10.1038/s41587-022-01302-5

17. Helmink BA, Reddy SM, Gao J, *et al*. B cells and tertiary lymphoid structures promote immunotherapy response. *Nature*. 2020;577(7791):549-555.

doi: 10.1038/s41586-019-1922-8

18. Petitprez F, de Reyniès A, Keung EZ, *et al*. B cells are associated with survival and immunotherapy response in sarcoma. *Nature*. 2020;577(7791):556-560. doi:10.1038/s41586-019-1906-8

19. Cabrita R, Lauss M, Sanna A, *et al*. Tertiary lymphoid structures improve immunotherapy and survival in melanoma. *Nature*. 2020;577(7791):561-565.

doi: 10.1038/s41586-019-1914-8

20. Williams HL, Frei AL, Koessler T, *et al*. The current landscape of spatial biomarkers for prediction of response to immune checkpoint inhibition. *NPJ Precis Oncol*. 2024;8(1):178.

doi: 10.1038/s41698-024-00671-1

21. Watson SS, Duc B, Kang Z, *et al*. Microenvironmental reorganization in brain tumors following radiotherapy and recurrence revealed by hyperplexed immunofluorescence imaging. *Nat Commun*. 2024;15(1):3226.

doi: 10.1038/s41467-024-47185-9

22. Liu W, Puri A, Fu D, *et al*. Dissecting the tumor microenvironment in response to immune checkpoint inhibitors via single-cell and spatial transcriptomics. *Clin Exp Metastasis*. 2024;41(4):313-332.

doi: 10.1007/s10585-023-10246-2

23. Dunn GP, Old LJ, Schreiber RD. The three Es of cancer immunoediting. *Annu Rev Immunol*. 2004;22:329-360.

doi: 10.1146/annurev.immunol.22.012703.104803

24. Koebel CM, Vermi W, Swann JB, *et al*. Adaptive immunity maintains occult cancer in an equilibrium state. *Nature*. 2007;450(7171):903-907.

doi: 10.1038/nature06309

25. Schreiber RD, Old LJ, Smyth MJ. Cancer immunoediting: Integrating immunity's roles in cancer suppression and promotion. *Science*. 2011;331(6024):1565-1570.

doi: 10.1126/science.1203486

26. Shankaran V, Ikeda H, Bruce AT, *et al*. IFNgamma and lymphocytes prevent primary tumour development and shape tumour immunogenicity. *Nature*. 2001;410(6832):1107-1111.

doi: 10.1038/35074122

27. Galon J, Costes A, Sanchez-Cabo F, *et al*. Type, density, and location of immune cells within human colorectal tumors predict clinical outcome. *Science*. 2006;313(5795):1960-1964.

doi: 10.1126/science.1129139

28. Mlecnik B, Tosolini M, Kirilovsky A, *et al*. Histopathologic-based prognostic factors of colorectal cancers are associated with the state of the local immune reaction. *J Clin Oncol*. 2011;29(6):610-618.

doi: 10.1200/jco.2010.30.5425

29. Hanahan D, Weinberg RA. Hallmarks of cancer: The next generation. *Cell*. 2011;144(5):646-674.

doi: 10.1016/j.cell.2011.02.013

30. Lu Q, Kou D, Lou S, *et al*. Nanoparticles in tumor microenvironment remodeling and cancer immunotherapy. *J Hematol Oncol*. 2024;17(1):16.

doi: 10.1186/s13045-024-01535-8

31. Zhang L, Zheng H, Jiang ST, *et al*. Worldwide research trends on tumor burden and immunotherapy: A bibliometric analysis. *Int J Surg*. 2024;110(3):1699-1710.

doi: 10.1097/js9.0000000000001022

32. Couzin-Frankel J. Breakthrough of the year 2013. Cancer immunotherapy. *Science*. 2013;342(6165):1432-1433.

doi: 10.1126/science.342.6165.1432

33. Maude SL, Frey N, Shaw PA, *et al*. Chimeric antigen receptor T cells for sustained remissions in leukemia. *N Engl J Med*. 2014;371(16):1507-1517.

doi: 10.1056/NEJMoa1407222

34. Geckin B, Konstantin Föhse F, Domínguez-Andrés J, Netea MG. Trained immunity: Implications for vaccination. *Curr Opin Immunol*. 2022;77:102190.

doi: 10.1016/j.coi.2022.102190

35. Quesada JR, Hersh EM, Manning J, *et al*. Treatment of hairy cell leukemia with recombinant alpha-interferon. *Blood*. 1986;68(2):493-497.

36. Andtbacka RH, Kaufman HL, Collichio F, *et al*. Talimogene laherparepvec improves durable response rate in patients with advanced melanoma. *J Clin Oncol*. 2015;33(25):2780-2788.

doi: 10.1200/jco.2014.58.3377

37. Fridman WH, Pagès F, Sautès-Fridman C, Galon J. The immune contexture in human tumours: Impact on clinical outcome. *Nat Rev Cancer*. 2012;12(4):298-306.

doi: 10.1038/nrc3245

38. Sun K, Xu Y, Zhang L, *et al*. A phase 2 trial of enhancing immune checkpoint blockade by stereotactic radiation and *in situ* virus gene therapy in metastatic triple-negative breast cancer. *Clin Cancer Res*. 2022;28(20):4392-4401.

doi: 10.1158/1078-0432.Ccr-22-0622

39. Wang XQ, Danenberg E, Huang CS, *et al*. Spatial predictors of immunotherapy response in triple-negative breast cancer. *Nature*. 2023;621(7980):868-876.

doi: 10.1038/s41586-023-06498-3

40. Yehan Z, Sheng Q, Hong Y, *et al*. To develop a prognostic model for neoadjuvant immunochemotherapy efficacy in esophageal squamous cell carcinoma by analyzing the immune microenvironment. *Front Immunol*. 2024;15:1312380.

doi: 10.3389/fimmu.2024.1312380

41. Wu C, Zhang G, Wang L, *et al*. Spatial proteomic profiling elucidates immune determinants of neoadjuvant chemo-immunotherapy in esophageal squamous cell carcinoma. *Oncogene*. 2024;43(37):2751-2767.

doi: 10.1038/s41388-024-03123-z

42. Lim CJ, Nguyen PHD, Wasser M, *et al*. Immunological hallmarks for clinical response to BCG in bladder cancer. *Front Immunol*. 2020;11:615091.

doi: 10.3389/fimmu.2020.615091

43. Xiao M, Tu L, Zhou T, He Y, Li X, Zuo Q. Predictive model based on multiple immunofluorescence quantitative analysis for pathological complete response to neoadjuvant immunochemotherapy in lung squamous cell carcinoma. *Front Oncol*. 2024;14:1396439.

doi: 10.3389/fonc.2024.1396439

44. Parra ER, Zhang J, Duose DY, *et al*. Multi-omics analysis reveals immune features associated with immunotherapy benefit in patients with squamous cell lung cancer from phase III lung-MAP S1400I trial. *Clin Cancer Res*. 2024;30(8):1655-1668.

doi: 10.1158/1078-0432.Ccr-23-0251

45. Berrell N, Monkman J, Donovan M, *et al*. Spatial resolution of the head and neck cancer tumor microenvironment to identify tumor and stromal features associated with therapy response. *Immunol Cell Biol*. 2024;102(9):830-846.

doi: 10.1111/imcb.12811

46. Hayes JD, Dinkova-Kostova AT, Tew KD. Oxidative stress in cancer. *Cancer Cell*. 2020;38(2):167-197.

doi: 10.1016/j.ccell.2020.06.001

47. Larroquette M, Guegan JP, Besse B, *et al*. Spatial transcriptomics of macrophage infiltration in non-small cell lung cancer reveals determinants of sensitivity and resistance to anti-PD1/PD-L1 antibodies. *J Immunother Cancer*. 2022;10(5):e003890.

doi: 10.1136/jitc-2021-003890

48. Monkman J, Kim H, Mayer A, *et al*. Multi-omic and spatial dissection of immunotherapy response groups in non-small cell lung cancer. *Immunology*. 2023;169(4):487-502.

doi: 10.1111/imm.13646

49. Peranzoni E, Lemoine J, Vimeux L, *et al*. Macrophages impede CD8 T cells from reaching tumor cells and limit the efficacy of anti-PD-1 treatment. *Proc Natl Acad Sci U S A*. 2018;115(17):E4041-E4050.

doi: 10.1073/pnas.1720948115

50. Leader AM, Grout JA, Maier BB, *et al*. Single-cell analysis of human non-small cell lung cancer lesions refines tumor classification and patient stratification. *Cancer Cell*. 2021;39(12):1594-1609.e12.

doi: 10.1016/j.ccell.2021.10.009

51. Park S, Ock CY, Kim H, *et al*. Artificial intelligence-powered spatial analysis of tumor-infiltrating lymphocytes as complementary biomarker for immune checkpoint inhibition in non-small-cell lung cancer. *J Clin Oncol*. 2022;40(17):1916-1928.

doi: 10.1200/jco.21.02010

52. Fan G, Xie T, Tang L, Li L, Han X, Shi Y. The co-location of CD14+APOE+ cells and MMP7+ tumour cells contributed to worse immunotherapy response in non-small cell lung cancer. *Clin Transl Med*. 2024;14(9):e70009.

doi: 10.1002/ctm2.70009

53. Ma J, Deng Y, Zhang M, Zhang Q. Spatial tertiary lymphoid structures imply response to anti-PD-1 plus anlotinib in advanced non-small cell lung cancer. *Immunology*. 2024;173:536-551.

doi: 10.1111/imm.13841

54. Moldoveanu D, Ramsay L, Lajoie M, *et al*. Spatially mapping the immune landscape of melanoma using imaging mass cytometry. *Sci Immunol*. 2022;7(70):eabi5072.

doi: 10.1126/sciimmunol.abi5072

55. Dammeijer F, van Gulijk M, Mulder EE, *et al*. The PD-1/PD-L1-checkpoint restrains T cell immunity in tumor-draining lymph nodes. *Cancer Cell*. 2020;38(5):685-700.e8.

doi: 10.1016/j.ccell.2020.09.001

56. Antoranz A, Van Herck Y, Bolognesi MM, *et al*. Mapping the immune landscape in metastatic melanoma reveals localized cell-cell interactions that predict immunotherapy response. *Cancer Res*. 2022;82(18):3275-3290.

doi: 10.1158/0008-5472.Can-22-0363

57. Gartrell RD, Marks DK, Hart TD, *et al*. Quantitative analysis of immune infiltrates in primary melanoma. *Cancer Immunol Res*. 2018;6(4):481-493.

doi: 10.1158/2326-6066.Cir-17-0360

58. Toki MI, Merritt CR, Wong PF, *et al*. High-plex predictive marker discovery for melanoma immunotherapy-treated patients using digital spatial profiling. *Clin Cancer Res*.

2019;25(18):5503-5512.

doi: 10.1158/1078-0432.Ccr-19-0104

59. Mi H, Ho WJ, Yarchoan M, Popel AS. Multi-scale spatial analysis of the tumor microenvironment reveals features of cabozantinib and nivolumab efficacy in hepatocellular carcinoma. *Front Immunol*. 2022;13:892250.

doi: 10.3389/fimmu.2022.892250

60. Huang CX, Lao XM, Wang XY, *et al*. Pericancerous cross-presentation to cytotoxic T lymphocytes impairs immunotherapeutic efficacy in hepatocellular carcinoma. *Cancer Cell*. 2024;42:2082-2097.e10.

doi: 10.1016/j.ccell.2024.10.012

61. Sheng J, Zhang J, Wang L, *et al*. Topological analysis of hepatocellular carcinoma tumour microenvironment based on imaging mass cytometry reveals cellular neighbourhood regulated reversely by macrophages with different ontogeny. *Gut*. 2022;71(6):1176-1191.

doi: 10.1136/gutjnl-2021-324339

62. Li Z, Pai R, Gupta S, *et al*. Presence of onco-fetal neighborhoods in hepatocellular carcinoma is associated with relapse and response to immunotherapy. *Nat Cancer*. 2024;5(1):167-186.

doi: 10.1038/s43018-023-00672-2

63. Sharma A, Seow JJW, Dutertre CA, *et al*. Onco-fetal reprogramming of endothelial cells drives immunosuppressive macrophages in hepatocellular carcinoma. *Cell*. 2020;183(2):377-394.e21.

doi: 10.1016/j.cell.2020.08.040

64. Sharma A, Blériot C, Currenti J, Ginhoux F. Oncofetal reprogramming in tumour development and progression. *Nat Rev Cancer*. 2022;22(10):593-602.

doi: 10.1038/s41568-022-00497-8

65. Wang H, Liang Y, Liu Z, *et al*. POSTN(+) cancer-associated fibroblasts determine the efficacy of immunotherapy in hepatocellular carcinoma. *J Immunother Cancer*. 2024;12(7):e008721.

doi: 10.1136/jitc-2023-008721

66. Liu Y, Xun Z, Ma K, *et al*. Identification of a tumour immune barrier in the HCC microenvironment that determines the efficacy of immunotherapy. *J Hepatol*. 2023;78(4):770-782.

doi: 10.1016/j.jhep.2023.01.011

67. Gil-Jimenez A, van Dijk N, Vos JL, *et al*. Spatial relationships in the urothelial and head and neck tumor microenvironment predict response to combination immune checkpoint inhibitors. *Nat Commun*. 2024;15(1):2538.

doi: 10.1038/s41467-024-46450-1

68. Reinstein ZZ, Zhang Y, Ospina OE, *et al*. Preexisting skin-resident CD8 and γδ T-cell circuits mediate immune response in Merkel cell carcinoma and predict immunotherapy efficacy. *Cancer Discov*. 2024;14(9):1631-1652.

doi: 10.1158/2159-8290.Cd-23-0798

69. Davidson G, Helleux A, Vano YA, *et al*. Mesenchymal-like tumor cells and myofibroblastic cancer-associated fibroblasts are associated with progression and immunotherapy response of clear cell renal cell carcinoma. *Cancer Res*. 2023;83(17):2952-2969.

doi: 10.1158/0008-5472.Can-22-3034

70. Gu X, Enane F, Tohme R, *et al*. PBRM1 loss in kidney cancer unbalances the proximal tubule master transcription factor hub to repress proximal tubule differentiation. *Cell Rep*. 2021;36(12):109747.

doi: 10.1016/j.celrep.2021.109747

71. Kieffer Y, Hocine HR, Gentric G, *et al*. Single-cell analysis reveals fibroblast clusters linked to immunotherapy resistance in cancer. *Cancer Discov*. 2020;10(9):1330-1351.

doi: 10.1158/2159-8290.Cd-19-1384

72. Tanaka M, Lum L, Hu K, *et al*. Tumor cell heterogeneity drives spatial organization of the intratumoral immune response. *J Exp Med*. 2025;222(6):e20242282.

doi: 10.1084/jem.20242282

73. Ma C, Yang C, Peng A, *et al*. Pan-cancer spatially resolved single-cell analysis reveals the crosstalk between cancer-associated fibroblasts and tumor microenvironment. *Mol Cancer*. 2023;22(1):170.

doi: 10.1186/s12943-023-01876-x

74. Tumeh PC, Harview CL, Yearley JH, *et al*. PD-1 blockade induces responses by inhibiting adaptive immune resistance. *Nature*. 2014;515(7528):568-571.

doi: 10.1038/nature13954

75. Gooden MJ, de Bock GH, Leffers N, Daemen T, Nijman HW. The prognostic influence of tumour-infiltrating lymphocytes in cancer: A systematic review with meta-analysis. *Br J Cancer*. 2011;105(1):93-103.

doi: 10.1038/bjc.2011.189

76. Yang Y, Attwood K, Bshara W, *et al*. High intratumoral CD8(+) T-cell infiltration is associated with improved survival in prostate cancer patients undergoing radical prostatectomy. *Prostate*. 2021;81(1):20-28.

doi: 10.1002/pros.24068

77. Gros A, Robbins PF, Yao X, *et al*. PD-1 identifies the patient-specific $CD8^+$ tumor-reactive repertoire infiltrating human tumors. *J Clin Invest*. 2014;124(5):2246-2259.

doi: 10.1172/jci73639

78. Simon S, Labarriere N. PD-1 expression on tumor-specific T cells: Friend or foe for immunotherapy? *Oncoimmunology*. 2017;7(1):e1364828.

doi: 10.1080/2162402x.2017.1364828

79. Weigelin B, den Boer AT, Wagena E, *et al*. Cytotoxic T cells are able to efficiently eliminate cancer cells by additive cytotoxicity. *Nat Commun*. 2021;12(1):5217.

doi: 10.1038/s41467-021-25282-3

80. Gide TN, Silva IP, Quek C, *et al*. Close proximity of immune and tumor cells underlies response to anti-PD-1 based therapies in metastatic melanoma patients. *Oncoimmunology*. 2020;9(1):1659093.

doi: 10.1080/2162402x.2019.1659093

81. Bocchialini G, Lagrasta C, Madeddu D, *et al*. Spatial architecture of tumour-infiltrating lymphocytes as a prognostic parameter in resected non-small-cell lung cancer. *Eur J Cardiothorac Surg*. 2020;58(3):619-628.

doi: 10.1093/ejcts/ezaa098

82. Nirmal AJ, Maliga Z, Vallius T, *et al*. The spatial landscape of progression and immunoediting in primary melanoma at single-cell resolution. *Cancer Discov*. 2022;12(6):1518-1541.

doi: 10.1158/2159-8290.Cd-21-1357

83. Zhang S, Deshpande A, Verma BK, *et al*. Informing virtual clinical trials of hepatocellular carcinoma with spatial multi-omics analysis of a human neoadjuvant immunotherapy clinical trial. *bioRxiv*; 2023. [Preprint].

doi: 10.1101/2023.08.11.553000

84. Aloisi F, Pujol-Borrell R. Lymphoid neogenesis in chronic inflammatory diseases. *Nat Rev Immunol*. 2006;6(3):205-217.

doi: 10.1038/nri1786

85. Drayton DL, Liao S, Mounzer RH, Ruddle NH. Lymphoid organ development: From ontogeny to neogenesis. *Nat Immunol*. 2006;7(4):344-353.

doi: 10.1038/ni1330

86. Sautès-Fridman C, Petitprez F, Calderaro J, Fridman WH. Tertiary lymphoid structures in the era of cancer immunotherapy. *Nat Rev Cancer*. 2019;19(6):307-325.

doi: 10.1038/s41568-019-0144-6

87. Gu-Trantien C, Loi S, Garaud S, *et al*. $CD4^+$ follicular helper T cell infiltration predicts breast cancer survival. *J Clin Invest*. 2013;123(7):2873-92.

doi: 10.1172/jci67428

88. Goc J, Germain C, Vo-Bourgais TK, *et al*. Dendritic cells in tumor-associated tertiary lymphoid structures signal a Th1 cytotoxic immune contexture and license the positive prognostic value of infiltrating CD8+ T cells. *Cancer Res*. 2014;74(3):705-715.

doi: 10.1158/0008-5472.Can-13-1342

89. Hennequin A, Derangère V, Boidot R, *et al*. Tumor infiltration by Tbet+ effector T cells and CD20+ B cells is associated with survival in gastric cancer patients. *Oncoimmunology*. 2016;5(2):e1054598.

doi: 10.1080/2162402x.2015.1054598

90. Kroeger DR, Milne K, Nelson BH. Tumor-infiltrating plasma cells are associated with tertiary lymphoid structures, cytolytic T-cell responses, and superior prognosis in ovarian cancer. *Clin Cancer Res*. 2016;22(12):3005-3015.

doi: 10.1158/1078-0432.Ccr-15-2762

91. Di Caro G, Bergomas F, Grizzi F, *et al*. Occurrence of tertiary lymphoid tissue is associated with T-cell infiltration and predicts better prognosis in early-stage colorectal cancers. *Clin Cancer Res*. 2014;20(8):2147-2158.

doi: 10.1158/1078-0432.Ccr-13-2590

92. McMullen TP, Lai R, Dabbagh L, Wallace TM, de Gara CJ. Survival in rectal cancer is predicted by T cell infiltration of tumour-associated lymphoid nodules. *Clin Exp Immunol*. 2010;161(1):81-88.

doi: 10.1111/j.1365-2249.2010.04147.x

93. Baratin M, Simon L, Jorquera A, *et al*. T cell zone resident macrophages silently dispose of apoptotic cells in the lymph node. *Immunity*. 2017;47(2):349-362.e5.

doi: 10.1016/j.immuni.2017.07.019

94. Barone F, Gardner DH, Nayar S, Steinthal N, Buckley CD, Luther SA. Stromal fibroblasts in tertiary lymphoid structures: A novel target in chronic inflammation. *Front Immunol*. 2016;7:477.

doi: 10.3389/fimmu.2016.00477

95. Fridman WH, Meylan M, Pupier G, Calvez A, Hernandez I, Sautès-Fridman C. Tertiary lymphoid structures and B cells: An intratumoral immunity cycle. *Immunity*. 2023;56(10):2254-2269.

doi: 10.1016/j.immuni.2023.08.009

96. Schumacher TN, Thommen DS. Tertiary lymphoid structures in cancer. *Science*. 2022;375(6576):eabf9419.

doi: doi:10.1126/science.abf9419

97. Fridman WH, Meylan M, Petitprez F, Sun CM, Italiano A, Sautès-Fridman C. B cells and tertiary lymphoid structures as determinants of tumour immune contexture and clinical outcome. *Nat Rev Clin Oncol*. 2022;19(7):441-457.

doi: 10.1038/s41571-022-00619-z

98. Kang J, Lee JH, Cha H, *et al*. Systematic dissection of tumor-normal single-cell ecosystems across a thousand tumors of 30 cancer types. *Nat Commun*. 2024;15(1):4067.

doi: 10.1038/s41467-024-48310-4

99. Meylan M, Petitprez F, Becht E, *et al*. Tertiary lymphoid structures generate and propagate anti-tumor antibody-producing plasma cells in renal cell cancer. *Immunity*. 2022;55(3):527-541.e5.

doi: 10.1016/j.immuni.2022.02.001

100. Xu Z, Wang Q, Zhang Y, *et al*. Exploiting tertiary lymphoid structures gene signature to evaluate tumor microenvironment infiltration and immunotherapy response in colorectal cancer. *Front Oncol*. 2024;14:1383096.

doi: 10.3389/fonc.2024.1383096

101. Glentis A, Oertle P, Mariani P, *et al*. Cancer-associated fibroblasts induce metalloprotease-independent cancer cell invasion of the basement membrane. *Nat Commun*. 2017;8(1):924.

doi: 10.1038/s41467-017-00985-8

102. Sun X, Wu B, Chiang HC, *et al*. Tumour DDR1 promotes collagen fibre alignment to instigate immune exclusion. *Nature*. 2021;599(7886):673-678.

doi: 10.1038/s41586-021-04057-2

103. Xiao Z, Tan Y, Cai Y, *et al*. Nanodrug removes physical barrier to promote T-cell infiltration for enhanced cancer immunotherapy. *J Control Release*. 2023;356:360-372.

doi: 10.1016/j.jconrel.2023.02.029

104. You R, Liu YP, Xie YL, *et al*. Hyperfractionation compared with standard fractionation in intensity-modulated radiotherapy for patients with locally advanced recurrent nasopharyngeal carcinoma: A multicentre, randomised, open-label, phase 3 trial. *Lancet*. 2023;401(10380):917-927.

doi: 10.1016/s0140-6736(23)00269-6

105. Tang R, Yin J, Liu Y, Xue J. FLASH radiotherapy: A new milestone in the field of cancer radiotherapy. *Cancer Lett*. 2024;587:216651.

doi: 10.1016/j.canlet.2024.216651

106. Pratx G, Kapp DS. Ultra-high-dose-rate FLASH irradiation may spare hypoxic stem cell niches in normal tissues. *Int J Radiat Oncol Biol Phys*. 2019;105(1):190-192.

doi: 10.1016/j.ijrobp.2019.05.030

107. Yang Y, Tian W, Su L, *et al*. Tumor-infiltrating cytotoxic T cells and tumor-associated macrophages correlate with the outcomes of neoadjuvant chemoradiotherapy for locally advanced rectal cancer. *Front Oncol*. 2021;11:743540.

doi: 10.3389/fonc.2021.743540

108. Lan J, Sun L, Xu F, *et al*. M2 macrophage-derived exosomes promote cell migration and invasion in colon cancer. *Cancer Res*. 2019;79(1):146-158.

doi: 10.1158/0008-5472.Can-18-0014

109. Zhang S, Li N, Wang F, *et al*. Characterization of the tumor microenvironment and identification of spatially predictive biomarkers associated with beneficial neoadjuvant chemoradiotherapy in locally advanced rectal cancer. *Pharmacol Res*. 2023;197:106974.

doi: 10.1016/j.phrs.2023.106974

110. Tian W, Yang Y, Qin Q, *et al*. Vimentin and tumor-stroma ratio for neoadjuvant chemoradiotherapy response prediction in locally advanced rectal cancer. *Cancer Sci*. 2023;114(2):619-629.

doi: 10.1111/cas.15610

111. Kaufmann J, Haist M, Kur IM, *et al*. Tumor-stroma contact ratio - a novel predictive factor for tumor response to chemoradiotherapy in locally advanced oropharyngeal cancer. *Transl Oncol*. 2024;46:102019.

doi: 10.1016/j.tranon.2024.102019

112. Chaib S, López-Domínguez JA, Lalinde-Gutiérrez M, *et al*. The efficacy of chemotherapy is limited by intratumoral senescent cells expressing PD-L2. *Nat Cancer*. 2024;5(3):448-462.

doi: 10.1038/s43018-023-00712-x

113. Verdaguer H, Saurí T, Acosta DA, *et al*. ESMO scale for clinical actionability of molecular targets driving targeted treatment in patients with cholangiocarcinoma. *Clin Cancer Res*. 2022;28(8):1662-1671.

doi: 10.1158/1078-0432.Ccr-21-2384

114. Kulasinghe A, Monkman J, Shah ET, Matigian N, Adams MN, O'Byrne K. Spatial profiling identifies prognostic features of response to adjuvant therapy in triple negative breast cancer (TNBC). *Front Oncol*. 2021;11:798296.

doi: 10.3389/fonc.2021.798296

115. O'Rourke CJ, Salati M, Rae C, *et al*. Molecular portraits of patients with intrahepatic cholangiocarcinoma who diverge as rapid progressors or long survivors on chemotherapy. *Gut*. 2024;73(3):496-508.

doi: 10.1136/gutjnl-2023-330748

116. Cai S, Zhao M, Yang G, *et al*. Modified spatial architecture of regulatory T cells after neoadjuvant chemotherapy in non-small cell lung cancer patients. *Int Immunopharmacol*. 2024;137:112434.

doi: 10.1016/j.intimp.2024.112434

117. Yang G, Hu M, Cai S, *et al*. Optimizing the spatial immune landscape of CD103(+)CD8(+) tissue-resident memory T cells in non-small cell lung cancer by neoadjuvant chemotherapy. *Cell Oncol (Dordr)*. 2024;47:1957-1971.

doi: 10.1007/s13402-024-00980-4

118. Huan X, Zou K, Zhang P, *et al*. Neoadjuvant chemotherapy is linked to an amended anti-tumorigenic microenvironment in gastric cancer. *Int Immunopharmacol*. 2024;127:111352.

doi: 10.1016/j.intimp.2023.111352

119. Zhao Y, Li D, Zhuang J, *et al*. Comprehensive multi-omics analysis of resectable locally advanced gastric cancer: Assessing response to neoadjuvant camrelizumab and chemotherapy in a single-center, open-label, single-arm phase II trial. *Clin Transl Med*. 2024;14(5):e1674.

doi: 10.1002/ctm2.1674

120. Bao X, Li Q, Chen D, *et al*. A multiomics analysis-assisted deep learning model identifies a macrophage-oriented module as a potential therapeutic target in colorectal cancer. *Cell Rep Med*. 2024;5(2):101399.

doi: 10.1016/j.xcrm.2024.101399

121. Shiau C, Cao J, Gregory MT, *et al*. Therapy-associated remodeling of pancreatic cancer revealed by single-cell spatial transcriptomics and optimal transport analysis. *bioRxiv*. 2023. [Preprint].

doi: 10.1101/2023.06.28.546848

122. Hwang WL, Jagadeesh KA, Guo JA, *et al*. Single-nucleus and spatial transcriptome profiling of pancreatic cancer identifies multicellular dynamics associated with neoadjuvant treatment. *Nat Genet*. 2022;54(8):1178-1191.

doi: 10.1038/s41588-022-01134-8

123. Zeng Z, Zhao Y, Chen Q, *et al*. Hypoxic exosomal HIF-1α-stabilizing circZNF91 promotes chemoresistance of normoxic pancreatic cancer cells via enhancing glycolysis. *Oncogene*. 2021;40(36):5505-5517.

doi: 10.1038/s41388-021-01960-w

124. Lin J, Xia L, Oyang L, *et al*. The POU2F1-ALDOA axis promotes the proliferation and chemoresistance of colon cancer cells by enhancing glycolysis and the pentose phosphate pathway activity. *Oncogene*. 2022;41(7):1024-1039.

doi: 10.1038/s41388-021-02148-y

125. Weinstein IB. Cancer. Addiction to oncogenes--the Achilles heal of cancer. *Science*. 2002;297(5578):63-64.

doi: 10.1126/science.1073096

126. Jin H, Wang L, Bernards R. Rational combinations of targeted cancer therapies: background, advances and challenges. *Nat Rev Drug Discov*. 2023;22(3):213-234.

doi: 10.1038/s41573-022-00615-z

127. Maemondo M, Inoue A, Kobayashi K, *et al*. Gefitinib or chemotherapy for non-small-cell lung cancer with mutated EGFR. *N Engl J Med*. 2010;362(25):2380-2388.

doi: 10.1056/NEJMoa0909530

128. McNamara KL, Caswell-Jin JL, Joshi R, *et al*. Spatial proteomic characterization of HER2-positive breast tumors through neoadjuvant therapy predicts response. *Nat Cancer*. 2021;2(4):400-413.

doi: 10.1038/s43018-021-00190-z

129. Coker EA, Stewart A, Ozer B, *et al.* Individualized prediction of drug response and rational combination therapy in NSCLC using artificial intelligence-enabled studies of acute phosphoproteomic changes. *Mol Cancer Ther*. 2022;21(6):1020-1029.

doi: 10.1158/1535-7163.Mct-21-0442

130. Zhou Tran Y, Minozada R, Cao X, *et al*. Immediate adaptation analysis implicates BCL6 as an EGFR-TKI combination therapy target in NSCLC. *Mol Cell Proteomics*. 2020;19(6):928-943.

doi: 10.1074/mcp.RA120.002036

131. De Angelis C, Nagi C, Hoyt CC, *et al*. Evaluation of the predictive role of tumor immune infiltrate in patients with HER2-positive breast cancer treated with neoadjuvant anti-HER2 therapy without chemotherapy. *Clin Cancer Res*. 2020;26(3):738-745.

doi: 10.1158/1078-0432.Ccr-19-1402

132. Valenza C, Guidi L, Battaiotto E, *et al*. Targeting HER2 heterogeneity in breast and gastrointestinal cancers. *Trends Cancer*. 2024;10(2):113-123.

doi: 10.1016/j.trecan.2023.11.001

133. Jiang L, Zhao X, Li Y, *et al*. The tumor immune microenvironment remodeling and response to HER2-targeted therapy in HER2-positive advanced gastric cancer. *IUBMB Life*. 2024;76(7):420-436.

doi: 10.1002/iub.2804

134. Zhang D, Ni Y, Wang Y, *et al*. Spatial heterogeneity of tumor microenvironment influences the prognosis of clear cell renal cell carcinoma. *J Transl Med*. 2023;21(1):489.

doi: 10.1186/s12967-023-04336-8

135. Zhang S, Yuan L, Danilova L, *et al*. Spatial transcriptomics analysis of neoadjuvant cabozantinib and nivolumab in advanced hepatocellular carcinoma identifies independent mechanisms of resistance and recurrence. *Genome Med*. 2023;15(1):72.

doi: 10.1186/s13073-023-01218-y

136. Arora R, Cao C, Kumar M, *et al*. Spatial transcriptomics reveals distinct and conserved tumor core and edge architectures that predict survival and targeted therapy response. *Nat Commun*. 2023;14(1):5029.

doi: 10.1038/s41467-023-40271-4

137. Ziemys A, Kim M, Menzies AM, *et al*. Integration of digital pathologic and transcriptomic analyses connects tumor-infiltrating lymphocyte spatial density with clinical response to BRAF inhibitors. *Front Oncol*. 2020;10:757.

doi: 10.3389/fonc.2020.00757

138. Siravegna G, Sartore-Bianchi A, Nagy RJ, *et al*. Plasma HER2 (ERBB2) copy number predicts response to HER2-targeted therapy in metastatic colorectal cancer. *Clin Cancer Res*. 2019;25(10):3046-3053.

doi: 10.1158/1078-0432.Ccr-18-3389

139. Marusyk A, Janiszewska M, Polyak K. Intratumor heterogeneity: The rosetta stone of therapy resistance. *Cancer Cell*. 2020;37(4):471-484.

doi: 10.1016/j.ccell.2020.03.007

140. Hou Y, Shen R, Chaudhary S, Gao F, Li Z. Correlation of expression of breast biomarkers in primary and metastatic breast carcinomas: A single-institution experience. *Acta Cytol*. 2016;60(5):481-489.

doi: 10.1159/000449400

141. Caswell-Jin JL, McNamara K, Reiter JG, *et al*. Clonal replacement and heterogeneity in breast tumors treated with neoadjuvant HER2-targeted therapy. *Nat Commun*. 2019;10(1):657.

doi: 10.1038/s41467-019-08593-4

142. Rye IH, Trinh A, Saetersdal AB, *et al*. Intratumor heterogeneity defines treatment-resistant HER2+ breast tumors. *Mol Oncol*. 2018;12(11):1838-1855.

doi: 10.1002/1878-0261.12375

143. Filho OM, Viale G, Stein S, *et al*. Impact of HER2 heterogeneity on treatment response of early-stage HER2-positive breast cancer: Phase II neoadjuvant clinical trial of T-DM1 combined with pertuzumab. *Cancer Discov*. 2021;11(10):2474-2487.

doi: 10.1158/2159-8290.Cd-20-1557